Nm23-H1 regulates contact inhibition of locomotion which is affected by ephrin-B1

Masamitsu Tanaka*, Sei Kuriyama and Namiko Aiba

From the Department of Molecular Medicine and Biochemistry, Akita University Graduate School of Medicine, 1-1-1 Hondo, Akita 010-8543, Japan

Running Title: Nm23H1 regulates contact inhibition of locomotion

*Address correspondence to: Masamitsu Tanaka, Tel. +81-018-884-6077; Fax. +81-018-884-6078; E-mail address: mastanak@med.akita-u.ac.jp

Abbreviations footnote: GST, glutathione S-transferase; GEF, guanine nucleotide exchange factor; aa, amino acid; i.c., intracranially ; RNAi, RNA interference

Keywords: Eph; ephrin; Nm23; contact inhibition; glioma

JCS online publication date 20 June 2012

Summary

Contact inhibition of locomotion (CIL) is the process by which cells stop the continual migration in the same direction after collision with another cell. Highly invasive malignant cells exhibit diminished CIL behavior when they contact with stromal cells, which allows stromal invasion of tumors. We show that Nm23-H1 is essential for the suppression of Rac1 through inactivation of Tiam1 at the sites of cell-cell contact, which plays a pivotal role in CIL. U87MG cells show CIL when they contact with normal glia. U87MG did not invade significantly into glias in spheroid confrontation assay, whereas reduction of Nm23-H1 expression in U87MG cells abrogates CIL and they invaded into glias. In U87MG cells, Nm23-H1 is translocated to the sites of contact with glia through association with α-catenin and N-cadherin. In the expression of wild type Nm23-H1, neither Nm23-H1 mutant, which lacks the binding ability with Tiam1, nor α-catenin recovered CIL. Moreover, the expression of ephrin-B1 in tumor cells disrupted CIL and promoted invasion. As one mechanism, ephrin-B1 inhibits the association of Nm23-H1 with Tiam1, which contributes for activation of Rac1. These results indicate a novel function of Nm23-H1 to control CIL, and its negative regulation by ephrin-B1.

Introduction

It is important to know the mechanism of invasion of malignant cells invade into normal stroma tissues. One mechanism is activation of metalloproteinases, which degrade surrounding extracellular substrates. In contrast, contact inhibition of locomotion (CIL) is the process by which cells disrupt or change their direction of migration upon contact with another cell (Mayor and Carmona-Fontaine, 2010). Malignant cells with high invasion potential exhibit diminished CIL behavior, which allows them to invade stromal tissues. Although the concept of CIL was first reported in the 1950's, the molecular mechanism of CIL is not well understood (Abercrombie and Heaysman et al. 1953). In our attempt to monitoring invasion of various glioblastoma cells into glias by cell culture, we observed that U87MG did not intermingle with normal glias and clear border of U87MG and glia was maintained when they conflict. On the other hand, some other glioblastoma cell line invaded into glias. Therefore, we particularly focused on the mechanism of invasion of these glioblastoma cells toward glias. In order to elucidate the mechanisms of cell invasion, regulation of Rac1 GTPase is essential for constructing membrane protrusions towards the direction of migration. Among the regulators of Rac1 activity, Tiam1 is a guanine nucleotide exchange factor (GEF) toward Rac1, which was originally identified in T lymphoma cells as an invasion and metastasis inducing gene (Habets et al. 1994). Tiam1 is also expressed in various cancer cells, and we previously observed that the GEF activity of Tiam1 is regulated by physical interaction with Nm23-H1 and ephrin-B1 (Tanaka et al. 2004; Otsuki et al. 2001).

Nonmetastatic protein 23 (Nm23) is a nucleotide diphosphate (NDP) kinase that is expressed from bacteria to mammals (Lacombe et al. 2000). In humans, there are eight members of the Nm23 family (Nm23-H1-8, respectively), of which Nm23-H1 and -H2 are most abundantly expressed (Boissan et al. 2009). Identified as the first metastasis suppressor, decreased expression of Nm23-H1 is associated with higher tumor grade and increased metastasis (Steeg et al. 2003). In contrast, exogenous expression of Nm23-H1 results in decreased migration, anchorage independent growth and metastasis in various cancer cells (Suzuki et al. 2004; Jung et al. 2006; McDermott et al. 2008). The metastasis

suppressive effect of Nm23-H1 was confirmed by Nm23 knockout mice, where the rate of tumor formation of hepatocellular carcinoma was unchanged; however, the knockout mice developed 2-fold more pulmonary metastases (Boissan et al. 2005). In addition to their nucleotide diphosphate kinase activity, members of this family have both histidine protein kinase and 3'-5' exonuclease (DNase) activities (Wagner et al. 1997; Fan et al. 2003). The protein histidine kinase activity of Nm23-H1 mediates the antimotility function *in vitro*, possibly via serine phosphorylation of the kinase suppressor of ras (KSR) and suppression of ras signaling (Hartsough et al. 2002). Recently, 3'-5' exonuclease activity was shown to be important for the Nm23-H1 metastasis suppressor function (Zhang et al. 2010). As one of the mechanisms by which Nm23-H1 suppresses cell migration, we previously observed that Nm23-H1 inhibits Rac1 activity through physical interaction with Tiam1 (Otsuki et al. 2001).

The members of the Eph receptor family can be classified into two groups based on their sequence similarity and their preferential binding to ligands tethered to the cell surface either by a glycosylphosphatidyl inositol-anchor (ephrin-A) or a transmembrane domain (ephrin-B) (Poliakov et al. 2004; Pasquale, 2008; Daar, 2011). Interaction of the Eph family of receptor protein tyrosine kinases and its ligand, ephrin family members, induces bi-directional signaling via cell-cell contacts. Overexpression of B-type ephrin in cancer cells correlates with high invasion and high vascularity of some tumors (Meyer et al. 2005; Castellvi et al. 2006) and elevated expression of ephrin-B1 is observed in poorly differentiated invasive tumor cells and other tumors with poor clinical prognosis (Kataoka et al. 2002; Varelias et al. 2002). Although investigation of the functions of Eph receptors and ephrins has focused on the development of the vascular and nervous systems, the roles of Eph-ephrin pathways in epithelial cells and cancers have also attracted interest (Batlle et al. 2005; Holmberg et al. 2006; Castano et al. 2008; Vaught et al. 2008). We previously observed that signaling through ephrin-B1 is involved in the promotion of carcinomatous peritonitis of gastric cancer and pancreas cancer (Tanaka et al. 2007a; 2007b; 2010).

In this report, we show that Nm23-H1 is required for CIL by suppression of Tiam1 activity at the sites of intercellular contacts between U87MG and glias. The C-terminus of Nm23-H1, which is required for association with α-catenin, was necessary for U87MG

cells to maintain CIL toward glia. In addition, ephrin-B1 inhibits the association of Nm23-H1 with Tiam1, which may be involved in tumor cell invasion into glias by affecting CIL. These results suggest that the regulation of intracellular localization of Nm23-H1 and its interaction with Tiam1 affects the stromal invasion of some types of cancer cells.

Results

Heterotypic CIL between U87MG and glia

In our attempt to study the mechanism of tumor cells invasion of mesenchymal tissues, spheroid confrontation assay, also called boundary assay was performed, where a co-culture is made using two different cells with each cell type occupying different territories with only a small gap separating the two cell fronts. As the cells divide and migrate, the two cellular fronts get closer to each other and finally collide. This allows the behavior of the two cellular populations to be analyzed at the boundary. Among several glioblastoma cell lines, U87MG showed a clear border of leading edges from those of glias, therefore they did not intermingle with each other (Fig. 1A). Invasion of tumor cells was evaluated as “invasion index”, which indicates percentage of invaded area in glial cell population (Supplementary 1A). When spheroids of tumor cells and glias were three dimensionally confronted on agarose coated plates, U87MG did not invade into the glial sphere (Fig 1B).

To further investigate the behavior of U87MG cells when they contact with glia, we performed time-lapse analysis in coculture system. When a free-moving U87MG cell came into contact with glia, its protrusion collapsed, the direction of its migration changed and moved away from glia (Fig 1C and Supplementary movie 1). We also performed time-lapse analysis in the spheroid confrontation assay where the cellular outgrowth of U87MG and glia met. U87MG promptly retracted protrusion or lamellipodium after contact with glia, and changed the direction of migration (Fig 1D and Supplementary movie 2). From the analysis of tracking migration of tumor cells, the persistence of cell migration increased after collision (Supplementary 2A, B). These observations suggest that contact inhibition of locomotion (CIL) occurred in U87MG cells after they collide with normal glias, which may lead to the little invasion of U87MG into glias in the spheroid

confrontation assay.

N-cadherin regulates CIL and invasion, and Nm23-H1 is accumulated in N-cadherin complex at cell-cell contacts.

In the recent analysis of developing embryos of Xenopus laevis, deprivation of N-cadherin abolished CIL in migrating neural crest cells (Theveneau et al. 2010). N-cadherin is a major cell adhesion molecule in glioblastomas and glia, and N-cadherin is located at the sites of contact between U87MG and glia (Fig 2A). Therefore, we examined whether N-cadherin was necessary for heterotypic CIL between U87MG and glia. Reduction of N-cadherin expression in U87MG cells and glias by RNA interference allowed tumor cells to invade glias (Fig. 2B, C). In order to show different planes of Z-stacks, pitched view of each X-Y plane was constructed, which also indicates intermingling of two cell populations is induced by reduction of N-cadherin (Supplementary 3). From the time-lapse analysis, N-cadherin silencing in U87MG inhibited retraction of the protrusion after collision with glia (Supplementary movie 3). These results suggest that N-cadherin is necessary for establishment of CIL and attenuates invasion of U87MG.

To next elucidate the mechanism of N-cadherin-mediated CIL and suppression of invasion, we focused on Nm23-H1. In recent report, Nm23-H1 makes a complex with N-cadherin through association with α-catenin (Aktary et al. 2010). In addition, we previously observed that Nm23-H1 physically interacts with Tiam1, a guanine nucleotide exchange factor toward Rac1, and prohibits the GEF activity of Tiam1. As Rac1 GTPase is important for the formation of cell membrane protrusions necessary for the forward cell movement, its regulation by Nm23-H1 at N-cadherin mediated cell-cell contacts may be important for establishment of CIL. Because Nm23-H1 and Tiam1 were expressed in U87MG and glia, we investigated the role of Nm23-H1 in the heterotypic CIL between these cells (Supplementary 4A). When localization of Nm23-H1 was examined in U87MG cells expressing EGFP-tagged Nm23-H1 under coculture with glias, Nm23-H1 was accumulated at the leading edge of the cell membrane contacting the glia, and also at the homotypic cell contacts between tumor cells (Supplementary 4B, left). In contrast, such accumulation of Nm23-H1 at the sites of cell-cell contact was scarcely observed in

N-cadherin deprived U87MG (Supplementary 4B, right). Furthermore, EGFP-tagged Nm23-H1 was accumulated at the cell membrane of U87MG contacting with microbeads coated with the extracellular domain of N-cadherin, but not control beads coated with mouse IgGFc (Supplementary 4D). These results indicate that Nm23-H1 is translocated to the site of cell-cell contacts after U87MG meets with glia, which largely depends on N-cadherin mediated adhesion complex.

The region of Nm23-H1 responsible for binding to α-catenin was next examined using deletion mutants of Nm23-H1. The mammalian Nm23 family consists of 152–168 aa and highly conserve each other. Diverse regions in the amino-terminus and carboxyl-terminus are called the V1 and V2 region, respectively (Iwashita et al. 2004). Based on this information, deletion mutants were constructed. From immunoprecipitation analysis, Nm23-H1-C, but not Nm23-H1-N binds to α-catenin, which indicates that the carboxyl-terminal region of Nm23-H1 was required to interact with α-catenin (Fig. 3A, B). In contrast, the C-terminal region of Nm23-H1 was not involved in the physical association with Tiam1 as Nm23-H1-N, which lacks the C-terminal region, still binds to Tiam1 as well as wild type Nm23-H1 (Fig. 3C). Moreover, the expression of Nm23-H1-N inhibited Tiam1 induced Rac1 activation in whole cell lysate examined by GTP-Rac1 pull down analysis (Fig. 3D). Therefore, these results indicate that Nm23-H1-N lacks binding ability with α-catenin, but can interact with Tiam1 and inhibits its'-GEF activity toward Rac1.

Association of Nm23-H1 with α-catenin is required for CIL and suppression of tumor invasion

We next examined whether recruitment of Nm23-H1 to N-cadherin mediated complex at cell-cell contacts is important for CIL between glioblastoma cells and glias. First, U87MG stably expressing Nm23-H1 miRNA was established, and then, reconstituted with wild type Nm23-H1 or Nm23-H1-N by transfection of miR-resistant rat ortholog of Nm23-H1 (Fig. 4, Top). The invasion of U87MG toward glia was examined by 2D or 3D sphere confrontation assay. U87MG cells in which Nm23-H1 was reduced (Nm23H1 miR) invaded the glia region (Fig. 4). The clear border between tumor cells and glia was recovered after wild type Nm23-H1, but not Nm23-H1-N was restored in Nm23H1 miR cells (Fig. 4, Supplementary 1B, C: Res Nm23-wt and –N, respectively). The intracellular

localization of EGFP-tagged Nm23-H1-N was further examined in U87MG cells. In contrast to the accumulation of wild type Nm23-H1 in the cell-cell contacts between U87MG and glia, EGFP-Nm23-H1-N diffusely existed in cytoplasm, and never located at intercellular contacts (Supplementary 4C). These results suggest that association with α-catenin is required for Nm23-H1 to accumulate to the site of cell-cell contact and suppress cell invasion.

To further evaluate the effects of Nm23-H1 on the invasion of tumor cells, time-lapse analysis was performed. After contact with glia, U87MG Nm23-H1 miR cell continued to move forward, and did not move away from the glia (Supplementary movie 4). In spheroid confrontation assay, migrating U87MG Nm23-H1 miR cell crossed over the glia and invaded into glial sphere (Supplementary movie 5). The CIL like movement of U87MG was restored by reconstitution of wild type Nm23-H1, but not Nm23-H1-N, suggesting that association of Nm23-H1 with α-catenin is necessary for maintain CIL (Supplementary movie 6, 7 and 8, respectively).

Nm23-H1 suppresses tumor invasion through association with Tiam1

Next, we examined whether interaction of Nm23-H1 with Tiam1 is important for regulation of tumor invasion. Recently, the unique acidic sequence motif necessary to associate with the PHCCEx region of Tiam1 and Tiam2 was identified in several molecules including ephrin-B1 and CD44, whose interaction was also reported in our previous study (Terawaki et al. 2010, Tanaka et al. 2004). When the sequence of Nm23-H1 was compared with Tiam1 binding motif of ephrin-B1$^{295\text{-}313}$ and CD44$^{713\text{-}730}$, Nm23-H1 amino acids (aa) 121–139 shares similarity (Fig. 5B). The critical residues in ExxE/DxxxxL of the acidic motif are conserved in Nm23-H1$^{121\text{-}139}$, and acidic residues of glutamates and aspartic acids are frequently present within this region. Association of wild type Nm23-H1 with PHCCEx of Tiam1 was detected by the immunoprecipitation analysis (Fig. 5C). Therefore, we prepared Nm23-H1 with mutation in two glutamates (E124, 127K; 2EK), whose corresponding residues in ephrin-B1 and CD44 are essential for binding with Tiam1. From immunoprecipitation analysis, the association of Nm23-H1$^{E124,\ 127K}$ (2EK) with Tiam1 was significantly decreased compared to wild type Nm23-H1 (Fig. 5D). Binding ability of Nm23-H1 with Tiam1 is required for Nm23-H1 to suppress invasion of U87MG cells,

because the reconstitution of Nm23-H1$^{E124, 127K}$ in U87MG Nm23-H1 miR cells did not inhibit tumor invasion into glias, and failed to suppress Rac1 activation (Fig. 5E middle, Fig. 5F: Res Nm23H1-2EK). In addition, reduction of Tiam1 expression suppressed Rac1 activation and invasion of Nm23-H1 deprived U87MG cells (Fig.5E right, Fig 5F: Nm23H1 miR+Tiam1 miR). These results suggest that Nm23-H1 prevents invasion of U87MG by suppression of Rac1 through controlling Tiam1.

Ephrin-B1 attenuates CIL by blocking physical association of Nm23-H1 with Tiam1.

We examined whether expression of ephrin-B1 affects CIL like behavior, and increases the invasion of tumor cells. Because U87MG expressed very low level ephrin-Bs, ephrin-B1 was stably overexpressed in this cell line (U87MG ephrin-B1) (Fig 6D). From the spheroid confrontation assay, U87MG expressing ephrin-B1 significantly invaded the area of glia cells (Fig. 6A, Supplementary 1B). The high potential of stromal invasion of U87MG ephrin-B1 was also observed by the assay where spheroids of tumor cells and glias were three dimensionally confronted on agarose coated plates. Many U87MG ephrin-B1 invaded the sphere of glia cells (Fig. 6B, Supplementary 1C). Consistent with these results, time-lapse analysis revealed that U87MG ephrin-B1 cell did not show repulsive CIL in both assays of single cells coculture and spheroid confrontation (Supplementary movie 9 and 10, respectively). In addition, U87MG cells expressing ephrin-B1 mutant, which lacks its cytoplasmic domain (Δcyt ephrin-B1), did not invade glias (Fig 6C left). Therefore, cytoplasmic region of ephrin-B1 is required for promoting cell invasion.

Rac1 activation of U87MG was increased by overexpression of either Tiam1 or ephrin-B1 (Fig. 6E). Expression of ephrin-B1 mutant, ephrin-B1 E297K, D300K, that lacks the binding capacity with Tiam1, did not affect Rac1 activation or invasion in spheroid confrontation assays (Fig. 6E, Fig. 6C middle). From time-lapse analysis, CIL was not affected by expression of ephrin-B1 E297K, D300K, either (Supplementary movie 11). These results suggest association with Tiam1 is necessary for ephrin-B1 mediated tumor invasion and disruption of CIL. On the other hand, knockdown of Tiam1 blocked Rac1 activation and invasion induced by ephrin-B1, suggesting that Rac1 activation following ephrin-B1 expression is mediated through Tiam1 (Fig. 6C right, Fig 6E: EFNB1 Tiam1 miR).

We next examined whether association of ephrin-B1 with Tiam1 attenuates the Tiam1-Nm23-H1 interaction. Association of Nm23-H1 with Tiam1 was inhibited by the expression of ephrin-B1 (Fig 7A). The association of endogenous Nm23-H1 with Tiam1 was also detected in U87MG, which was much reduced by overexpression of ephrin-B1 (Fig 7B). Moreover, treatment of cells with the peptide corresponding to the binding motif of ephrin-B1 with Tiam1 (ephrin-B1 295-313) also blocked interaction of Tiam1 with Nm23-H1, and induced Rac1 activation and invasion of tumor cells (Supplementary 5A). Intracellular delivery of the peptides was confirmed by immunostaining of the cells with anti-TAT antibody (data not shown). These results suggest that ephrin-B1 and Nm23-H1 competitively associate with Tiam1, and overexpression of ephrin-B1 sequesters Tiam1 from Nm23-H1.

We further examined the stromal invasion of glioblastoma cells endogenously expressing ephrin-B1 at high level; i.e. C6 cell line, and revealed that C6 and glia cells diffusely intermingled with each other (Fig 7C, upper). When ephrin-B1 of C6 was reduced by miRNA, C6-glia intermingling was inhibited (Fig 7C, bottom). In time-lapse analysis, most of wild type C6 cells remained attach to glia after they contact, whereas C6 ephrin-B1 miR cells changed the direction and moved away from glia (Supplementary movie 12, 13). In addition, silencing of ephrin-B1 in C6 increased association of Nm23-H1 with Tiam1, and suppressed Rac1 activation (Fig 7D, E). These results suggest that ephrin-B1 on the cell surface plays pivotal roles in tumor cell invasion by the mechanism including suppression of CIL.

Ephrin-B1 increases peripheral invasion of glioblastoma cells *in vivo*.

To further examine whether ephrin-B1 affects tumor invasion *in vivo*, tumors of ephrin-B1 overexpressed U87MG or ephrin-B1 reduced C6 in mice brain were compared with those of corresponding parent cells. The tumor of parent U87MG cells exclusively expanded in the brain with a relatively clear margin, while the margin of the tumor of ephrin-B1 overexpressed U87MG cells was irregularly shaped (Fig 8A). Irregularity of the tumor periphery was evident in group of ephrin-B1 overexpression (Table 1), which was also confirmed by tracing the tumor margin and quantified (Materials and Methods, Supplementary 2C). In addition, parent C6 cells invaded into cerebral tissue with irregular

tumor periphery, whereas tumor of C6 ephrin-B1miR cells was less invasive with relatively clear tumor margin (Fig 8B). Expression of ephrin-B1 in these transplanted tumors was also confirmed by immunohistochemistry (Fig 8A, B bottom panels). Although we did not observe significant difference of tumor size between the groups of wild type and overexpression (U87MG) or knock down (C6) of ephrin-B1, survival rate was decreased by expression of ephrin-B1 (Table 1). These results indicate the expression of ephrin-B1 promotes the peripheral invasion of some glioblastoma cells *in vivo*.

Discussion

In this study, we focused on the invasion of brain tumor cells after they confront normal glias. In order to examine the invasion of tumor cells into normal cells, spheroid confrontation assay is often performed (Golembieski et al. 1999; Rosenzweig et al. 2006). Among the cell lines derived from glioblastoma, U87MG cells did not enter into the sphere of glias by this confrontation assay. The mild invasion of U87MG cells into glias or normal fetal brain aggregates was also observed by others using a similar method (Golembieski et al. 1999; Rosenzweig et al. 2006). From time-lapse imaging, the protrusion of U87MG was retracted after contact with glia, and new lamellipodia or protrusions were produced in opposite direction, and then, U87MG moved away from glia. This behavior matches the CIL, a process that stop the continual locomotion of a cell in the same direction after collision with another cell. Therefore, we used U87MG as a model of the CIL of tumor cells toward stromal cells. The parameters of CIL were analyzed in various time-lapse images of single cell coculture, and plotted in Supplementary 2B. The frequency of CIL was also estimated by counting tumor cells, which moved back and away from glia during 1 hr after collision (Table 2). From these results, the degree of tumor cells invasion in spheroid confrontation assay was well correlated with disturbance of CIL.

We showed that Nm23-H1 plays a pivotal role in heterotypic CIL between parent U87MG and glia, which requires the interaction of Nm23-H1 with Tiam1 at the sites of intercellular contacts. As one of the mechanisms of recruitment of Nm23H1 to cell-cell contacts, it associates with α-catenin and N-cadherin, and inhibits local activation of Tiam1, which may suppress the formation of membrane protrusions toward glia (Supplementary

7A). Ephrin-B1 disrupts CIL via activation of Tiam1, which at least partly depends on the mechanism that attenuates Nm23-H1-Tiam1 interaction (Supplementary 7B).

The inhibitory effect of Nm23-H1 on cell migration and invasion was reported in some tumors (Boissan et al. 2010). We also observed increased motility and Rac1 activation in whole cell lysate of Nm23-H1 deprived U87MG (Supplementary 5C and data not shown). Therefore, Nm23-H1 may be involved in the suppression of cell movements through downregulation of total Rac1 activation. However, the result where Nm23-H1 mutant unable to associate with α-catenin (Nm23-H1-N) did not rescue CIL without losing its function as Tiam1 inhibitor indicates that recruitment of Nm23-H1 to the site of cell-cell contact is required for Nm23-H1 to cause CIL, and suggests that localized Rac1 activation at the intercellular contact is important for regulation of CIL.

Nm23-H1 has at least three functions as NDP kinase, histidine kinase and 3'-5' exonuclease. However, Nm23-H1 mediated CIL is unlikely to correlate with these functions. We observed that Nm23-H1 K12Q, which has recently been reported to abrogate all these three functions of Nm23-H1, did not apparently affect the CIL of U87MG toward glias (data not shown) (Zhang et al. 2010). In contrast, the C-terminal region of Nm23-H1 was required for maintaining the CIL of U87MG cells. Therefore, establishment of CIL through the C-terminus of Nm23-H1 may be a novel mechanism of Nm23 to suppress tumor invasion. This C-terminal portion contains the V2 region, which is diverse in the Nm23 family. Among Nm23-H1 to –H8, the V2 region of Nm23-H1 is conserved more in Nm23-H2 (76% amino acids identity), and less in Nm23-H3 (42% identity). Therefore, Nm23-H1 and –H2 may preferentially contribute to the establishment of CIL.

Recent studies of cell migration of cranial neural crest (CNC) cells, a highly migratory and multipotent embryonic cell population, demonstrate that the directional migration of CNC cells *in vivo* is regulated by CIL, and N-cadherin plays a pivotal role during CIL (Carmona-Fontaine et al. 2008; Theveneau et al. 2010). Defect of CIL by reduction of N-cadherin in U87MG and glias implicates that N-cadherin mediated cell-cell communication is also important for the establishment of CIL between tumor cells and stromal cells. In addition, Nm23-H1 may interact with several intercellular adhesion molecules besides N-cadherin through α-catenin. For example, E-cadherin also makes a

complex with α-catenin and Nm23-H1 (Aktary et al. 2010). It should be elucidated whether Nm23-H1 also makes a complex with other adhesion molecules, and is involved in regulation of the CIL of other types of cancers.

Cell repulsion is a well known effect of Eph/ephrin interaction (Pasquale, 2008; Genander and Frisen, 2010; Poliakov et al. 2004). When an Eph expressing cell meets another cell expressing cognate ephrin, they move in the opposite direction, which is the cell behavior of CIL. In recent report, EphA and ephrin-A mediates homotypic CIL of prostate cancer cells, whereas the forward signaling of EphBs in cancer cells disrupts CIL between cancer cell and fibroblast (Astin et al. 2010). Therefore, we examined expression and activation of several Ephs in confrontation assay of U87MG and glia. Among EphA4, EphA5 and EphB2, which were detected as major Eph receptors in U87MG by RT-PCR and western blotting, we did not detect apparent activation of any of these receptors by coculture with glia, whereas activation of EphB2 was observed when ephrin-B1 overexpressed U87MG was cocultured with glia as expected (Supplementary 6). Although the evidence of Eph receptors' activation was not obtained, we cannot rule out activation of other Ephs or ephrins expressed low level in U87MG may cause repulsive CIL after contact with glia. It should be further elucidated whether Nm23-H1 modifies Eph/ephrin mediated cell repulsion by interacting with them.

Extracellular interaction of EphB receptors activates ephrin-B1 signaling in tumor cells, which may also affect CIL and invasion, as we observed EphB2 expression in glia. However, membrane permeable peptide of ephrin-B1, which binds to Tiam1 (ephrin-B1$^{295\text{-}313}$), disrupted invasion of U87MG and activated Rac1 as well as wild type ephrin-B1 (Supplementary 5A). Therefore, association with Tiam1 may be enough for ephrin-B1 to cause invasion, although some other mechanisms may have additional effects. An increase of *in vivo* invasion of U87MG cells was also reported by overexpression of ephrin-B2 (Nakada et al. 2010). As ephrin-B1, -B2 and –B3 share a conserved motif necessary for binding to Tiam1, all these B-type ephrins may affect interaction of Tiam1 with Nm23-H1, and -H2, and regulate CIL behavior in malignancies.

This study suggests that ephrin-B1 contributes to the local activation of Rac1 via sequestration of Tiam1 from its inhibitor Nm23-H1. Besides that, certain possibilities of

ephrin-B1 mediated Rac1 activation may be considered. For example, physical association of ephrin-B1 may alter conformation of Tiam1 and affect its activity, or ephrin-B1 may modify the interaction of N-cadherin with β- and α-catenin at cell-cell contacts. However, we do not have any evidence at present that ephrin-B1 directly activates the GEF activity of Tiam1, and overexpression of ephrin-B1 did not affect the physical interaction of N-cadherin with β- and α-catenin (data not shown). As one of the mechanisms of ephrin-B1 mediated enhancement of cancer cell invasion, we previously reported that the C-terminus of ephrin-B1 regulates the exocytosis of matrix metalloproteinase (MMP) through the activation of Arf1 GTPase (Tanaka et al. 2007). We detected elevation of MMP-1 and slight increase of collagen invasion of U87MG cells overexpressing ephrin-B1 (Supplementary 5B, D). However, elevation of MMP-1 was also detected in U87MG cells expressing ephrin-B1 E297K, D300K, which did not affect CIL or invasion of U87MG (Supplementary 5D, Supplementary movie 11). Therefore, if activation of MMP-1 contributes for invasion of ephrin-B1 overexpressed U87MG, it does not seem to play a major role in this assay. On the other hand, CIL of C6 ephrin-B1miR cell was rather low frequency, and parameters of angle θ and persistence suggested relatively mild CIL was induced comparing to U87MG. Therefore, some other mechanisms besides CIL may also modify invasion of tumor cells, especially C6 cells in the spheroid confrontation assay.

This study revealed a novel function of Nm23-H1 for the establishment of CIL. Although we focused on the CIL of heterotypic cells between tumor and glia to investigate the mechanism of stromal invasion of tumors, Nm23-H1 may also play a central role in homotypic CIL of various normal cells. In addition to the known enzymatic activities, Nm23-H1 C-terminus mediated regulation of CIL is considered to contribute to metastasis suppressor activity.

MATERIALS AND METHODS

Plasmids, antibodies and reagents

Plasmids encoding full-length cDNAs of human ephrin-B1 and Nm23-H1 were previously described (Tanaka et al. 2007a; Otsuki et al. 2001). Rat cDNA of Nm23-H1 was PCR amplified from cDNA synthesized from rat kidney. Mutant forms of Nm23-H1 lacking the

amino terminus (C, aa37 to 152) or carboxyl terminus (N, aa 1- 138) were generated by PCR-based techniques, and cloned into pCS2 with or without six copies of myc-epitope tag at amino-terminus. Ephrin-B1$^{E297K,\ D300K}$ and Nm23-H1$^{E124,\ 127K}$ were generated by Site-Directed Mutagenesis kit (Stratagene, Santa Clara, CA, USA). PHCCEx region of human Tiam1 was described (Tanaka et al. 2004). To generate the recombinant retrovirus, cDNA was subcloned into a pDON-AI vector (Takara, Tokyo, Japan). N-cadherin-Fc was constructed by fusing the extracellular region of murine N-cadherin$^{1-725}$ with Fc region of mouse IgG2b. N-cadherin-Fc fusion protein was purified from the culture medium of COS1 cells transfected with plasmids encoding N-cadherin-Fc using a Protein G sepharose column as described previously (Tanaka et al. 2005) Rabbit polyclonal antibody that recognizes conserved C-terminal region of ephrin-B1, -B2 and –B3 (C18) was purchased from Santa Cruz Biotechnology, Inc. (SantaCruz, CA, USA) The goat polyclonal antibody against ephrin-B1, which reacts with the entire extracellular domain, was purchased from R&D Systems (Minneapolis, MN, USA). Polyclonal antibody for Nm23-H1 and MMP-1 was purchased from SantaCruz and Millipore, respectively. Monoclonal antibody for N-cadherin, which reacts to cytoplasmic region of N-cadherin was purchased from BD Biosciences. Monoclonal antibodies for N-cadherin, HA-epitope and myc-epitope (9E10) were purchased from BD Biosciences (Franklin Lakes, NJ, USA), BAbCO (Richmond, CA, USA) and Santa Cruz, respectively. Ephrin-B1$^{295-313}$ peptide was synthesized as a fusion peptide of membrane permeable domain of HIV-TAT as follows: GRKKRRQRRRPPQGGGAGTEPSDIIIPLRTTENNY. As a control, the scrambled sequence peptide that contains the same aa composition was synthesized: GRKKRRQRRRPPQGGGETLITIYERPGADNTSPIN.

Preparation of N-cadherin-Fc-coated beads

Latex-sulfate microspheres (5.2 μm diameter; International Dynamics Corporation) were coated with N-cadherin-Fc fusion protein according to the procedure described (Tanaka et al. 2005). Briefly, beads were suspended in 0.1M borate buffer, pH8.0, and incubated with goat anti-mouse IgG (Fc-specific) antibody (ICN, Aurora, OH, USA). After the beads were washed with PBS, the beads were then incubated with N-cadherin-Fc protein. After the incubation, the beads were washed for three times with PBS, and resuspended in PBS

containing 5 mg/ml bovine serum albumin (BSA).

Cell culture and transfection

Glioblastoma cell lines used in this study were obtained from the American Type Culture Collection (Rockville, MD, USA). Glias were isolated from the brains of E14 Wistar rat fetuses. Briefly, brains were aseptically dissected, placed in dishes containing DMEM and meningeal coverings were removed. Then, the brains were dissociated with 0.025% trypsin by pippeting. The single cells were transferred into DMEM containing 10% FBS, gentamycin (0.1mg/ml), penicillin (100 U/ml) and streptomycin (100 mg/ml). U87MG cell line and COS1 cells were cultured in DMEM supplemented with 10% fetal bovine serum. For transient expression assays, COS1 cells were transfected with plasmid DNA using FuGene6 reagent (Invitrogen, Carlsbad, CA, USA). Recombinant retroviral plasmid, pDON-AI was cotransfected with pCL-10A1 retrovirus packaging vector (IMGENEX, San Diego CA, USA) into 293gp cells to allow the production of retroviral particles (Tanaka et al. 2007a). U87MG cells stably overexpressing ephrin-B1 was established after retrovirus infection through the selection in medium containing G418 (600 μg/ml). In some experiments, peptides were added to the cultured cells at the final concentration of 5 μM.

Construction of siRNA and miR RNAi vectors

A system stably expressing miRNA was generated using the BLOCK-iT PolII miR RNAi expression vector kit (Invitrogen) according to the manufacturer's instructions. In the generation of the miR RNAi vectors for Nm23-H1, N-cadherin and Tiam1, following forward primers were used. Nm23-H1, 5'-TGCTGAATGAAGGTACGCTCACAGTTGTTTTGGCCACTGACTGACAACTGTG AGTACCTTCATT-3'; N-cadherin#1, 5'-TGCTGTTCACCAGAAGCCTCTACAGAGTTTTGGCCACTGACTGACTCTGTAG ACTTCTGGTGAA-3'. N-cadherin#2, 5'-TGCTGTGAAGATACCAGTTGGAGGCTGTTTTGGCCACTGACTGACAGCCTCC ATGGTATCTTCA-3'. Tiam1, 5'-TGCTGAAAGCTCGCCGTCTCCATGAAGTTTTGGCCACTGACTGACTTCATGGA CGGCGAGCTTT-3'.

U87MG stably expressing the miRNA vector for Nm23-H1 was established and cultured in

medium containing blasticidin (Invitrogen) at a concentration of 10 μ g/ml for 3 weeks. Small interfering RNAs (siRNA) of rat N-cadherin were synthesized as follows (CosmoBio, Tokyo Japan). Rat N-cadherin sense #1: 5'-CCAUCAAACCUGUGGGAAU-3'; Rat N-cadherin sense #2: 5'- CCGCAAGAGCUUGUCAGAA-3'; The control siRNA (scramble II duplex) was purchased from Dharmacon. siRNAs were incorporated into rat glia cells with Lipofectamine RNAiMax according to the manufacturer's instructions (Invitrogen).

Spheroid confrontation assay

Spheroid confrontation assay was performed basically as described with some modifications (Golembieski et al. 1999). Briefly, glias were labeled in green fluorescent 3,3'-dioctadecycloxacarbo-cyanine perchlorate (DiO) dye and tumor cells were labeled in the red fluorescent 1,1'-dioctadecyl-3,3,3',3'-tetramethyllindo-carbocyanine perchlorate (DiI) dye according to the manufacturer's instruction (Invitrogen). The fluorescent labeled cells were detached with trypsin, and each $3X10^5$ cells were collected in the complete growth medium and cultured in 6 well plates coated with 1% agarose gel for overnight to make spheroids of cell aggregates. In case of 3D confrontation assay, the glia and tumor aggregates were brought into contact by means of a sterile needle in 96 well plates coated with 1% agarose gel. After 72 hrs incubation, the fused aggregates were fixed in 4% paraformaldehyde, and sealed with a coverslip on a glass slide. When the confrontation assay was performed in 2D culture condition, aggregates of glia and tumor cells were randomly plated on new 24 well plates coated with fibronectin (20 μg/ml), and continued incubation for 12 hrs until the cells outgrowing from each aggregates meet each other. The invasion of tumor spheroids into the normal glia aggregate was observed by confocal microscope (LSM510, Zeiss). Among z-stack images of each sample, the single plane with maximal intermingling of glia and tumor cells was selected. In cases that no evident invasion was observed, the single plane of middle Z-position was shown. In some cases, each X-Y plane of Z-stacks was pitched by "3D cut view" menu (LSM510, Zeiss) to show the images in different planes together (Supplementary 6).

Live cell imaging

Prior to imaging glias and tumor cells were labeled with DiO and DiI, respectively.

Collisions of tumor cells and glia were analyzed by phase-contrast time-lapse microscopy with the 40x objective for up to 8 hrs (37℃, 5% CO_2) (BZ-9000, Keyence). Fluorescence views were taken prior to start imaging in order to distinguish glia and tumor cell. When time-lapse analysis was performed in the spheroid confrontation assay, images were taken by multi-acquisition phase-contrast time-lapse microscopy with the 20x objective at 10 min intervals for up to 24 hrs (37℃, 5% CO_2). The images were analyzed by tracking migration of tumor cells using Image J software and Manual tracking plugin. The positions of the collision (at t) between tumor cell and glial cell were determined manually, and the positions at the appropriate time-point before (t-Δt) and after (t+Δt) the collision were also determined. Basically, Δt is 1 hr. The angle θ was calculated from these points. Persistence before and after collision was determined from the direct distances between the points divided by actual distances of the entire trip during Δt. The nucleus was used as a marker to track, however, the protrusion was tracked in some cases when displaced distance of protrusion was larger than that of nucleus. Both of them were correlated (e.g. Supplementary movie 4, 6, 12).

Invasion index and statistical analysis

To quantify how much the glioma cells (labeled red) invaded into glial cells (labeled green) the fluorescent images were analyzed by Image J software. The invasion index (I) was calculated as the ratio (percentage) of overlapping glioma area (invaded red: iR) to glial cell area (total green: tG). I (%) = iR/tG x 100. At least three assays were performed for each sample, and invasion index was shown as mean +/- SD.

Immunoprecipitation and immunoblotting

Cell lysates were prepared with protease inhibitors in PLC buffer [50 mM Hepes (pH 7.5), 150-mM NaCl, 1.5-mM $MgCl_2$, 1-mM EGTA, 10% glycerol, 100-mM NaF, 1-mM Na_3VO_4 and 1% Triton X-100]. To precipitate the proteins, 1 μg of monoclonal or affinity purified polyclonal antibody was incubated with 500 μg of cell lysate for 2 hrs at 4°C, and then precipitated with protein G agarose for 1 hr at 4°C. Immunoprecipitates were extensively washed with PLC buffer, separated by SDS-PAGE, and immunoblotted.

Cell migration assay

Migration assay was performed using Transwell chambers with a polycarbonate nucleopore

membrane (BD Falcon, Franklin Lakes, NJ). Filters (8-μm pore size) were rehydrated with 100 μl of medium. Then, $1x10^4$ cells in 200 μl of serum-free medium were seeded onto the upper part of each chamber, whereas the lower compartment were filled with 600 μl of the same medium with 10% fetal bovine serum (FBS). After incubation for 8 hrs at 37℃, nonmigrated cells on the upper surface of the filter were wiped out with a cotton swab, and the migrated cells on the lower surface of the filter were fixed and stained with Giemsa's stain solution. The totals of migrated cells were determined by counting cells in five microscopic fields per well, and the extent of migration was expressed as the average number of cells per microscopic field. The assays were performed three times.

Rac1-GTP pull-down assay

The activation of Rac1 was examined by affinity precipitation of GTP-bound Rac1 with the GST-fusion protein of the p21-binding domain of PAK1 (GST-PBD) as described (Otsuki et al, 2001). Briefly, cell lysates were prepared in lysis buffer [50-mM Hepes (pH 7.5), 150-mM NaCl, 10-mM $MgCl_2$, 10% glycerol, 100-mM NaF, 1-mM Na_3VO_4 and 1% Triton X-100], and then, incubated with gluthathione-Sepharose beads containing a GST-PBD fusion protein for 45 min at 4°C. Precipitates were washed four times in the same buffer, and the precipitated GTP-bound Rac1 was detected by immunoblotting. Band intensities were quantified by Image J software, and the amount of GTP-Rac1 was normalized by total Rac1. Experiments were repeated for three times.

In vivo intracranial dissemination assay

All animal experimental protocols were approved by the Committee for Ethics of Animal Experimentation, and the experiments were conducted in accordance with the guidelines for Animal Experiments in Akita University. Intracranial dissemination of tumors was tested by i.c. injection of $2 x10^5$ tumor cells suspended in 30 μl of DMEM medium into 6-week-old BALB/c nude mice (n=10, each). The mice were sacrificed 12 days after injection and subjected to histopathological examination of the tumors. To examine survival rate, tumor cells were inoculated in another set of mice as above, and evaluated 21 days later. To quantify irregularity of tumor expansion in mice brain, HE stained section was photographed, and the images were analyzed by Image J software. The boundaries were determined by thresholding of the color density of the tissues, and the edge points were

manually tracked. We picked a few random points (B) and the fixed positions at the end of the image (A,C) on the invasive edge, and draw the rectangle and the circumscribed circle (CC) of it (Supplementary 1C). The diameter of CC (R) is calculated from the distances between three points (formula 1). The center angle of the minor arc between A and C is calculated by the length of AC and R (formula 2). The length of the minor arc (Lc) is determined by the diameter and the center angle (formula 3). We calculated the total length of the edge-line from the trajectory of the image (La). The irregular index (Ir) is defined by La/Lc. For instance, when any B is on the CC Ir becomes 1, which means the smooth boundary between tumor and the invaded tissues.

Immunocytochemical staining

Immunocytochemical staining was performed as previously described (Tanaka et al. 2005). In some experiments, the coverglasses were coated with fibronectin. For transfection, 5.0 x 10^4 cells were seeded on a glass and then fixed in 4% paraformaldehyde and stained. The staining was visualized using a confocal microscopic system (Zeiss).

Immunohistochemical analysis

Tumor tissues in the brain of nude mice were fixed, and embedded in paraffin. Paraffin blocks were sectioned in slices and subjected to immunohisotochemical staining using the indirect polymer method with Envision reagent (DAKO, Carpinteria, CA). Antigen retrieval was performed by placing sections in the citrate buffer and autoclaved according to the manufacturer's instructions.

Acknowledgments

This work was supported by a Grant-in-Aid for Cancer Research from the Ministry of Education, Culture, Science and Technology of Japan, the National Cancer Center Research and Development Fund and in part by a Grant of The Uehara Memorial Foundation, The Naito Foundation and The Yasuda Medical Foundation.

Conflict of interest

The authors declare that they have no conflict of interest.

References

Abercrombie M. and Heaysman J.E.M. (1953) Observations on the social behavior of cells in tissue culture: I. Speed of movement of chick heart fibroblasts in relation to their mutual contacts. Exp Cell Res 5, 111-131

Aktary Z., Chapman K., Lam L., Lo A., Ji C., Graham K., Cook L., Li L., Mackey JR. and Pasdar M. (2010) Plakoglobin interacts with and increases the protein levels of metastasis suppressor Nm23-H2 and regulates the expression of Nm23-H1. Oncogene 29, 2118–2129

Astin JW., Batson J., Kadir S., Charlet J., Persad RA., Gillatt D., Oxley JD. and Nobes CD.(2010) Competition amongst Eph receptors regulates contact inhibition of locomotion and invasiveness in prostate cancer cells Nature Cell Biol. 12, 1194-1204

Batlle, E., Bacani, J., Begthel, H., Jonkheer, S., Gregorieff, A., Van den Born, M., Malats, N., Sancho, E., Boon, E., Pawson, T., Gallinger, S., Pals, S. and Clevers, H. (2005) EphB receptor activity suppresses colorectal cancer progression. Nature 435, 1126-1130.

Boissan M,Wendum D, Arnaud-Dabernat S, Munier A, Debray M, Lascu I, Daniel JY, Lacombe ML. (2005) Increased lung metastasis in transgenic NM23-Null/SV40 mice with hepatocellular carcinoma. J Natl Cancer Inst 97, 836-845.

Boissan M, Dabernat S, Peuchant E, Schlattner U, Lascu I, Lacombe ML. (2009) The mammalian Nm23/NDPK family: from metastasis control to cilia movement. Mol Cell Biochem. 329, 51-62

Boissan M., De Wever O., Lizarraga F., Wendum D., Poincloux R., Chignard N., Desbois-Mouthon C., Dufour S., Nawrocki-Raby N, Birembaut P., Bracke M., Chavrier P., Gespach C. and Lacombe M. (2010) Implication of metastasis suppressor NM23-H1 in maintaining adherens junctions and limiting the invasive potential of human cancer cells. Cancer Res. 70, 7710–7722

Castano J., Davalos V., Schwarz Jr S. and Arango D. (2008) Eph receptors in cancer. Histol Histopathol 23, 1011-1023.

Carmona-Fontaine C., Mattews HK., Kuriyama S., Moreno M., Dunn GA., Parsons M., Stern CD. And Mayor R. (2008) Contact inhibition of locomotion in vivo controls neural crest directional migration Nature 456, 957-961

Castellvi, J., Garcia, A., De la Torre, J., Hernandez, J., Gil, A., Xercavins, J. and Cajal, SR. (2006) EphrinB expression in epithelial ovarian neoplasms correlates with tumor differentiation and angiogenesis. Human Pathology 37, 883-889.

Daar I. (2011) Non-SH2/PDZ reverse signaling by ephrins. Semin Cell Dev Biol (in press).

Fan Z., Beresford PJ., Oh DY., Zhang D., Lieberman J. (2003) Tumor suppressor NM23-H1 is a granzyme A-activated DNase during CTL-mediated apoptosis, and nucleosome assembly protein SET is its inhibitor. Cell 112, 659-672

Golembieski WA., Ge S., Nelson K., Mikkelsen T. and Rempel SA. (1999) Increased SPARC expression promotes U87 glioblastoma invasion in vitro Int. J. Devl Neuroscience 17, 463-472

Habets G.G., Scholtes E.H., Zuydgeest D., van der Kammen R.A., Stam J.C., Berns A. and Collard J.G. (1994) Identification of an invasion-inducing gene, Tiam-1, that encodes a protein with homology to GDP-GTP exchangers for Rho-like proteinsCell 77, 537-549

Hartsough MT., Morrison DK., Salerno M., Palmieri D., Outas T, Mair M., Patrick J. and Steeg PS. (2002) Nm23-H1 metastasis suppressor phosphorylation of kinase suppressor of Ras via a histidine protein kinase pathway. J Biol Chem 277, 32389-32399

Holmberg. J., Genander, M., Halford, MM., Anneren, C., Sondell, M., Chumley, MJ., Silvany, RE., Henkemeyer, M., Frisen, J. (2006) EphB receptors coordinate migration and proliferation in the intestinal stem cell niche. Cell 125, 1151-1263.

Iwashita S., Fujii M., Mukai H., Ono Y. and Miyamoto M. (2004) Lbc proto-oncogene product binds to and could be negatively regulated by metastasis suppressor nm23-H2 Biochem Biophy Res Commun 320, 1063–1068

Jung S., Paek YW., Moon KS., Wee SC., Ryu HH., Jeong YI. (2006) Expression of Nm23 in gliomas and its effect on migration and invasion in vitro. Anticancer Res 26, 249-258

Kataoka, H., Tanaka, M., Kanamori, M., Yoshii, S., Ihara, M., Wang, YJ., Song, JP., Li, ZY., Arai, H., Otuki, Y., Kobatashi, T., Kohno, H., Hanai, H. and Sugimura, H. (2002) Expression profile of EFNB1, EFNB2, two ligands of EPHB2 in human gastric cancer. J Cancer Res Clin Oncol. 128, 343-348.

Lacombe ML., Milon L., Munier A., Mehus JG., Lambeth DO. (2000) The human Nm23/nucleoside diphosphate kinases. J Bioenerg Biomembr 32, 247-258

Maret D., Gruzglin E., Seyed Sadr M., Siu V., Shan W., Koch A.W. Seidah N.G., Del Maestro R.F. and Colman D.R. (2010) N-cadherin promotes tumor cell invasion. Neoplasia 12, 1066-1080.

Mayor R and Carmona-Fontaine C. (2010) Keeping in touch with contact inhibition of locomotion Trends in Cell Biology 20, 319-328

McDermott WG., Boissan M., Lacombe ML., Steeg PS., Horak CE. (2008) Nm23-H1 homologs suppress tumor cell motility and anchorage independent growth. Clin Exp Metastasis 25, 131-138

Meyer, S., Hafner, C., Guba, M., Flegel, S., Geissler, EK., Becker, B., Koehl, G., Orso, E., Landthaler, M. and Vogt, T. (2005) Ephrin-B2 overexpression enhances integrin-mediated ECM-attachment and migration of B16 melanoma cells. Int. J. Oncol. 27, 1197-1206.

Nakada M., Anderson EM., Demuth T., Nakada S., Reavie LB., Drake KL., Hoelzinger DB. and Berens ME. (2010) The phosphorylation of ephrin-B2 ligand promotes glioma cell migration and invasion Int J. Cancer: 126, 1155–1165

Otsuki Y., Tanaka M., Yoshii S., Kawazoe N., Nakaya K. and Sugimura H. (2001) Tumor metastasis suppressor nm23H1 regulates Rac1 GTPase by interaction with Tiam1 Proc Natl Acad Sci 98, 4385-4390

Pasquale, EB. (2008) Eph-ephrin bidirectional signaling in physiology and disease. Cell 133, 38-52

Poliakov, A., Cotrina, M. and Wilkinson, DG. (2004) Diverse roles of Eph receptors and ephrins in the regulation of cell migration and tissue assembly. Dev Cell 7, 465-480.

Rosenzweig T., Ziv-Av A., Xiang C., Lu W., Cazacu S., Taler D., Miller CG., Reich R., Shoshan Y., Anikster Y., Kazimirsky G., Sarid R. and Brodie C. (2006) Related to Testes-Specific, Vespid, and Pathogenesis Protein-1 (RTVP-1) is overexpressed in gliomas and regulates the growth, survival, and invasion of glioma cells Cancer Res 66, 4139-4148

Steeg PS., Ouatas T., Halverson D., Palmieri D., Salermo M. (2003) Metastasis suppressor genes: basic and potential clinical use Clin Breast Cancer 4, 51-62

Suzuki E., Ota S., Ysukada K., Okita A., Matsuoka K., Murakami M. (2004) Nm23-H1

reduces in vitro cell migration and the liver metastatic potential of colon cancer cells by regulating myosin light chain phosphorylation. Int J Cancer 108, 207-211

Tanaka, M., Ohashi, R., Nakamura, R., Shinmura, K., Kamo, T., Sakai, R. and Sugimura, H. (2004) Tiam1 mediates neurite outgrowth induced by ephrin-B1 and EphA2. The EMBO J. 23, 1075-1088.

Tanaka, M., Kamata, R. and Sakai, R. (2005) Phosphorylation of ephrin-B1 via the interaction with claudin following cell-cell contact formation. The EMBO J. 24, 3700-3711.

Tanaka M., Sasaki K., Kamata R., Sakai R. (2007a) The C-terminus of ephrin-B1 regulates metalloproteinase secretion and invasion of cancer cells. J Cell Sci. 120, 2179-2189.

Tanaka M., Kamata, R., Takigahira, M., Yanagihara, K., Sakai, R. (2007b) Phosphorylation of ephrin-B1 regulates dissemination of gastric scirrhous carcinoma. Am J Pathol.; 171, 68-78.

Tanaka M, Kamata R, Yanagihara K and Sakai R. (2010) Suppression of gastric cancer dissemination by ephrin-B1-derived peptide. Cancer Science 101, 87-93

Terawaki S., Kitano K., Mori T., Zhai Y., Higuchi Y., Itoh N.,Watanabe T., Kaibuchi K. and Hakoshima T. (2010) The PHCCEx domain of Tiam1/2 is a novel protein- and membrane-binding module The EMBO Journal 29, 236–250

Theveneau E., Marchant L., Kuriyama S., Gull M., Moepps B., Parsons M. and Mayor R. (2010) Collective chemotaxis requires contact-dependent cell polarity Dev Cell 19, 39-53

Valster A., Tran NL., Nakada M., Berens ME., Chan AY., Symons M. (2005) Cell migration and invasion assays. Methods 37, 208-215

Varelias, A., Koblar, SA., Cowled, PA., Carter, CD. and Clayer, M. (2002) Human osteosarcoma express specific ephrin profiles: implications for tumorigenicity and prognosis. Cancer 95, 862-869.

Vaught D., Brantley-Sieders DM. and Chen J. (2008) Eph receptors in breast cancer: roles in tumor promotion and tumor suppression. Breast Cancer Res 10, 217-224.

Wagner PD., Steeg PS., Vu ND. (1997) Two-component kinase-like activity of nm23 correlates with its motility-suppressing activity. Proc Natl Acad Sci 94, 9000-9005

Zhang Q., McCorkle J.R., Novak M., Yang M. and Kaetzel M. (2010) Metastasis

suppressor function of NM23-H1 requires its 3’-5’ exonuclease activity Int J Cancer 128, 40-50

Figure legends

Fig. 1 (A, B) Spheroid confrontation assay was performed using rat glia with U87MG on fibronectin coated coverslips (A), or on agarose coated 96 well plates (B) as described in Materials and Methods. Bar= 20 μm. Glia cells and tumor cells were labeled with DiO (green) and DiI (red), respectively. In B, the corresponding computer-reconstructed vertical sections in the X-Z or Y-Z plane were attached. I (%) indicates invasion index as described in Materials and Methods. (C, D) Representative time-lapse microscopy images of U87MG/glia collision at the indicated times were shown. (C: Supplementary movie 1) Single cells of U87MG (marked with yellow and red asterisks) and glia (green asterisk) were cocultured. The arrows indicate the moving direction of U87MG marked with the same colored asterisk. Bar= 50 μm. (D: Supplementary Movie 2) Spheroid confrontation assay was performed as in A. Red colored cells are U87MG. Bar= 50 μm. Dotted line indicates the periphery of glias.

Fig. 2 N-cadherin mediates CIL between U87MG and glia. (A) Glia expressing EGFP and U87MG cells were cocultured. Cells were immunostained with anti-N-cadherin antibody (red). Bar= 10 μm. Asterisk indicates the position of U87MG cell. (B) Expression of N-cadherin was reduced in U87MG and glia by transfection of RNAi of human or rat N-cadherin, respectively. Band intensities were quantified and relative expression level was calculated. (C) Spheroid 3D confrontation assay was performed with either control or N-cadherin reduced cells of U87MG and glia on agarose coated 96 well plates. N-cadherin RNAi#1 indicates confrontation between U87MG expressing miRNA#1 and glia expressing siRNA#1. Glia cells and tumor cells were labeled with DiO (green) and DiI (red), respectively. Number below the panel indicates invasion index. Bar= 20 μm.

Fig. 3 C-terminus of Nm23-H1 physically associates with α-catenin. (A) A schematic diagram of wild type and deletion mutants of Nm23-H1 used in this study. “RNAi” indicates the position of miRNA used in Fig. 4. “121-141” indicates the region of sequence depicted in Fig. 5B. (B, C) Physical association of Nm23-H1 with α-catenin and Tiam1. Cos1 cells were transiently transfected with N-terminally myc-tagged wild type (wt) or

truncated Nm23-H1 together with N-terminally flag-tagged α-catenin (B) or Tiam1 (C), as indicated. (B) Nm23-H1 was immunoprecipitated (IP) with anti-myc antibody, and coprecipitated α-catenin was detected by anti-flag antibody. Asterisk indicates immunoglobulin H chain. (C) Tiam1 was immunoprecipitated by anti-Tiam1 antibody and coprecipitated Nm23-H1 was detected by anti-myc antibody. It should be noted that six copies of myc-epitope tagged with the Nm23-H1 cDNA increases the protein size around 9 KDa. Arrowheads indicate coprecipitated wild type or mutant of Nm23-H1. (D) Cos1 cells were transfected with Tiam1 with or without deletion mutants of Nm23-H1, as indicated. Cells were lysed for affinity precipitation with immobilized GST-PBD. Precipitated endogenous GTP-bound Rac1 was detected by immunoblotting. Band intensities were quantified, and normalized intensities were calculated relative to control cells (lane 1). Data are means +/- SD (n=3). * $P < 0.01$ versus control (lane 1).

Fig. 4 Association of Nm23-H1 with α-catenin is required for CIL. Top: U87MG cells were stably transfected with control miR (cont) or Nm23-H1 miR (Nm23H1miR). ResNm23H1 wt and ResNm23H1-N indicates Nm23-H1 rescue clones which reconstituted in Nm23H1miR cell with untagged wild type Nm23-H1 or Nm23-H1-N, respectively. Expression of Nm23-H1 in each cell line was examined by immunoblotting with anti-Nm23-H1 antibody. Bottom: Spheroid confrontation assay of DiO labeled glias (green) and DiI labeled various U87MG cell lines (red) was performed at 2D culture on fibronectin coated glass or 3D condition on agarose coated plates, as described in Fig. 2. Bar= 20 μm. Number below the panel indicates invasion index.

Fig. 5 Association of Nm23-H1 with Tiam1 is required for CIL. (A) Domains in Tiam1. PH-CC-Ex region contains an N-terminal Pleckstrin homology (PHn) domain, a putative coiled-coil (CC) region and a conserved extra (Ex) region. PDZ; PSD-95/DlgA/ZO-1 domain. DH; Dbl homology domain. PHc; C-terminal PH domain. (B) Sequence alignment of PHCCEx-binding region of human ephrin-B1 and CD44 with human or rat Nm23-H1$^{121–141}$. Critical residues for binding to PHCCEx are marked by asterisks. Acidic residues are in red. (C) Cos1 cells were transiently transfected with N-terminally

flag-tagged PHCCEx of Tiam1 with or without C-terminally HA-tagged Nm23-H1. Nm23-H1 was immunoprecipitated with anti-HA, and PHCCEx was detected by anti-flag antibody. Asterisk indicates immunoglobulin L chain. (D) Cos1 cells were transfected with HA-tagged wild type Nm23-H1 (wt) or Nm23-H1$^{E124,\ 127K}$ (2EK) together with or without Tiam1. Tiam1 was immunoprecipitated, and Nm23-H1 was detected by anti-HA antibody. (E) Spheroid 3D confrontation assay of DiO labeled glias and DiI labeled U87MG rescue mutant of Nm23-H1$^{E124,\ 127K}$ (2EK) or U87MG double knock down of Nm23-H1 and Tiam1 (Nm23-H1 miR+Tiam1 miR) was performed. Bar= 20 μm. (F) Rac1 activation (GTP-Rac1) was assayed in various U87MG cell lines as indicated. Bands intensities were quantified and normalized intensities were calculated relative to control cells (lane 1). Data are means+/- SD (n=3). * P< 0.01 versus control (lane 1).

Fig.6 Heterotypic CIL between U87MG and glia was abolished by expression of ephrin -B1. (A, B) Spheroid confrontation assay was performed using glia (green) with U87MG ephrin-B1 cells (red) on fibronectin coated coverslips (A), or on agarose coated 96 well plates (B) as in Fig.1. Bar= 20 μm. (C) Spheroid 3D confrontation assay of glias (green) and U87MG stably expressing cytoplasmic domain deleted ephrin-B1 (Δcyt EFNB1), ephrin-B1$^{E297K,\ D300K}$ or ephrin-B1 together with Tiam1 miRNA (Ephrin-B1 Tiam1 miR) was performed. Expression of wild type (wt) and Δcyt ephrin-B1 was shown by Western blotting using the antibody reacts to the extracellular domain of ephrin-B1. Bar= 20 μm.
(D) Expression level of ephrin-Bs in various glioblastoma cell lines was examined by immunoblotting with anti-pan ephrin-B antibody as described in Materials and Methods. (E) Rac1 activation (GTP-Rac1) was assessed in various U87MG cell lines as indicated. Band intensities were quantified, and normalized intensities were calculated relative to control cells (lane 1). Data are means +/- SD (n=3). * P< 0.01 versus parent U87MG (lane 1).

Fig.7 Effects of ephrin-B1 and Nm23-H1 on CIL are via regulation of Tiam1. (A) Cos1 cells were cotransfected with C-terminally HA-tagged Nm23-H1 and Tiam1 with or without ephrin-B1. Cells were lysed for IP with anti-Tiam1 which were then subject to

immunoblot (IB) with anti-HA to detect Nm23-H1. Band intensities (marked by arrowhead) were quantified, and relative ratio of the amount of precipitated Nm23-H1 was calculated. Data are means +/- SD (n=3). * P< 0.01 (B) Lysate prepared from wild type or ephrin-B1 overexpressed U87MG was subjected for immunoprecipitation with anti-Tiam1 antibody or control rabbit IgG. Coprecipitated Nm23-H1 was detected by immunoblot with anti-Nm23H1 antibody. (C) C6 glioblastoma cells invade into glias. Top: Spheroid confrontation assay on fibronectin-coated coverslips revealed significant intermingling of C6 and glias. Bottom: Invasion of C6 cells was inhibited by reduction of ephrin-B1. Bar= 10 μm. * P< 0.01 versus control. (D) Tiam1 was immunoprecipitated from lysate prepared from wild type or ephrin-B1 reduced C6. Coprecipitated Nm23-H1 was detected by immunoblot with anti-Nm23H1 antibody. Data are means +/- SD (n=3). * P< 0.01 (E) Rac1 activation was assessed in wild type or ephrin-B1 reduced C6 cells. Band intensities were quantified, and normalized intensities were calculated relative to control cells (lane 1). Data are means +/- SD (n=3). * P< 0.01

Fig.8 Ephrin-B1 increases peripheral invasion of glioblastoma cells in brain. (A) Control U87MG mock transfected cells or U87MG ephrin-B1 cells (A), or control C6 or C6 ephrin-B1miR cells (B) were injected intracranially into nude mice ($2x10^5$/mouse). Five mice were analyzed for each group and repeated twice. Representative histology of mice cerebrum 12days after injection of tumor cells is shown by H&E stain (upper) and immunohistochemistry with goat anti ephrin-B1 antibody (bottom). T indicates area occupied by tumor cells. Tumors in the same location were analyzed for irregularity (Ir) of tumor margin. *P< 0.01 versus control. Bar= 500 μm. Two clones of each U87MG ephrin-B1 or C6 ephrin-B1miR were examined and similar results were obtained.

Supplementary 1 (A) Example of quantification of invasion index of 2D (a) or 3D (b) confrontation assay. (B, C) Statistical analysis of 2D (B) or 3D (C) spheroid confrontation assays. Invasion index was calculated as described in Materials and Methods. At least three assays were performed for each sample, and invasion index was shown as means +/- SD. * P< 0.01 versus control.

Supplementary 2 (A) Analysis of CIL by tracking cell migration. The displacement trajectories before (AB) and after (BC) the collision. Red lines (Trip) indicate the actual trajectories of the cell. The angle θ and persistence were calculated as described in Materials and Methods. (B) The angle θ and change of persistence after collision (determined as P_{BC} / P_{AB}) of supplementary movies were plotted. When angle θ is small and persistence increased after collision (P_{BC} / P_{AB} > 1), which means repulsive CIL. (C) Quantification of irregularity of tumor margin in mice brain.

Supplementary 3 Z-stacks of spheroid 3D confrontation assay. Each plane of Z-stacks of Fig 2 (left and middle panel) was pitched as demonstrated above panels and displayed together (also described in Materials and Methods). White lines indicate the region where tumor cells invaded into glial cell population. Bar= 20 μm.

Supplementary 4 (A) Western blot of Tiam1 and Nm23-H1 in U87MG, C6 and rat glia. (B) EGFP-tagged Nm23-H1 was transiently transfected in U87MG parent cells (left) or U87MG stably expressing N-cadherin miRNA#1 (right). (C) Parent U87MG cells were transiently transfected with EGFP-tagged Nm23-H1-N. (B, C) The tumor cells were cocultured with DiI-labeled glia cells (red). The cells were fixed, and visualized using a confocal microscopic system. Dotted line in A indicates the periphery of adjacent untransfected U87MG cell. Concentrated Nm23-H1 localization at the contact site with glia was indicated by arrows. Bar= 10 μm. (D) Microbeads precoated with N-cadherin-Fc or control Fc were added to U87MG cells transfected with EGFP-tagged Nm23-H1. After 30 min incubation, cells were fixed and visualized using a confocal microscopic system. To visualize beads, photos were taken as merged image of fluorescence and differential interference contrast (Dic). The positions of the beads were marked with asterisk. High magnification of boxed area was shown in islets (fluorescence view without Dic). Bar= 10 μm.

Supplementary 5 (A) U87MG cells were treated with the peptide of

ephrin-B1$^{295\text{-}313}$ or scrambled control peptide (5 μM). Association of Tiam1 and Nm23-H1 was examined by immunoprecipitation of Tiam1 (upper left), and activation of Rac1 was assessed by affinity precipitation with GST-PBD (upper right). Invasion of U87MG into glia was examined by spheroid confrontation assay (middle panels). (B) Migration and invasion through type I collagen matrix of parent or ephrin-B1 overexpressed U87MG was assayed by Transwell. (C) Transwell assay examining migration of Nm23-H1 deprived U87MG. (B, C) Number of migrated cells on the bottom surface of the Transwell membrane was counted. The results from three independent experiments, each in duplicate, are shown as the mean +/- SD. *P<0.01. (D) Left: Gelatin zymography of conditioned medium of U87MG parent cells, U87MG ephrin-B1, U87MG Nm23-H1 miR cells and U87MG expressing ephrin-B1E297K, D300K. Coomassie stained gel was shown. Right: Western blot of MMP-1 in culture medium of indicated cells.

Supplementary 6 Spheroid confrontation assay (2D CIL assay) was performed as described in the manuscript. Cell lysate was prepared from spheroids of U87MG or glia alone, or confronted spheres (e.g. U87wt + glia). Equal volume of lysate was subjected for immunoprecipitation of each Eph, and then immunoblotted with anti phosphotyrosine antibody. Densitometric analysis of relative phosphorylation level was shown. Data are means +/- SD (n=3). * P< 0.01 versus parent U87MG (pY EphB2).

Supplementary 7 Diagram showing the possible mechanism of Nm23-H1 mediated CIL. (A) In response to contact of U87MG cell with glia, Nm23-H1 is recruited to the sites of intercellular contacts including the complex of N-cadherin and α-catenin. Interaction of Nm23-H1 with Tiam1 suppresses GEF activity of Tiam1 toward Rac1, which prevents formation of forward membrane protrusions. (B) Ephrin-B1 promotes invasion of tumor cell by the mechanisms including disruption of CIL through suppression of Nm23-H1 / Tiam1 interaction.

Supplementary movie legends

Movie 1 Parent U87MG and glia (yellow arrow) collision. Coculture of single

cells. Frames taken every 70 sec. Bar= 50 μm.

Movie 2 Parent U87MG (red) and glia (green) collision. Spheroid confrontation assay. Frames taken every 10 min. Bar= 50 μm. Representative cell movement was tracked. Arrows point the positions of collision.

Movie 3 U87MG-N-cadherin-miRNA#1 and glia (yellow arrow). Coculture of single cells. Frames taken every 80 sec. Bar= 50 μm.

Movie 4 U87MG-Nm23-H1-miRNA and glia (yellow arrow). Coculture of single cells. Frames taken every 68 sec. Bar= 50 μm.

Movie 5 U87MG-Nm23-H1-miRNA (red) and glia (green). Spheroid confrontation assay. Frames taken every 10 min. Bar= 50 μm. Arrows point the positions of collision.

Movie 6 U87MG-ResNm23-H1-wt (wild type Nm23-H1 was reconstituted in Nm23-H1-miR cell) and glia (yellow arrow). Coculture of single cells. Frames taken every 68 sec. Bar= 50 μm.

Movie 7 U87MG-ResNm23-H1-wt (red) and glia (green). Spheroid confrontation assay. Frames taken every 10 min. Bar= 50 μm. Arrows point the positions of collision.

Movie 8 U87MG-ResNm23-H1-N (red) and glia (green). Spheroid confrontation assay. Frames taken every 10 min. Bar= 50 μm. Arrows point the positions of collision.

Movie 9 U87MG ephrin-B1 and glia (yellow arrow). Coculture of single cells. Frames taken every 70 sec. Bar= 50 μm. The tip of tumor cell reached to the opposite side of glia.

Movie 10 U87MG ephrin-B1 (red) and glia (green). Spheroid confrontation assay.

Frames taken every 10 min. Bar= 50 µm.

Movie 11 U87MG ephrin-B1$^{E297K,\ D300K}$ (red) and glia (green). Spheroid confrontation assay. Frames taken every 10 min. Bar= 50 µm.

Movie 12 C6 (wild type) and glia (yellow arrow). Coculture of single cells. Frames taken every 106 sec. Bar= 50 µm.

Movie 13 C6 ephrin-B1miR and glia (yellow arrow). Coculture of single cells. Frames taken every 106 sec. Bar= 50 µm.

Table 1

Incidence of mice bearing tumor with irregularly shaped margin

	# irregular margin/ # bearing tumor[1, 2]	# surviving/ # transplanted[1]	# surviving/ # transplanted[3]
U87MG Control	0/8	9/10	6/10
U87MG Ephrin-B1	8/8	8/10	2/10
C6 Control	8/8	8/10	1/10
C6 ephrin-B1miR	3/10	10/10	6/10

[1] Result of 12 days afer inoculation of tumor cells

[2] Number of mice containing tumor with irregularly shaped margin (Ir > 3.0)/ number of mice bearing tumor

[3] Number of mice survived 21 days after inoculation of tumor cells

Table 2

	Inidence of CIL (%) [1]	n [2]
U87 MG		
Wild type	70.0	30
N-cadherin miR(#1)	13.3	30
Nm23-H1miR	12.5	32
Res Nm23-H1 wt	70.0	30
Res Nm23-H1-N	13.3	30
Ephrin-B1	10.0	30
Ephrin-B1$^{E297K, D300K}$	66.7	30
C6		
Wild type	6.7	30
Ephrin-B1 miR	46.7	30

[1]Percentage of tumor cells moved back ($\theta < 90$) and away from glia during 1hr after collision

[2] Number of cells analyzed

Fig 1 A B

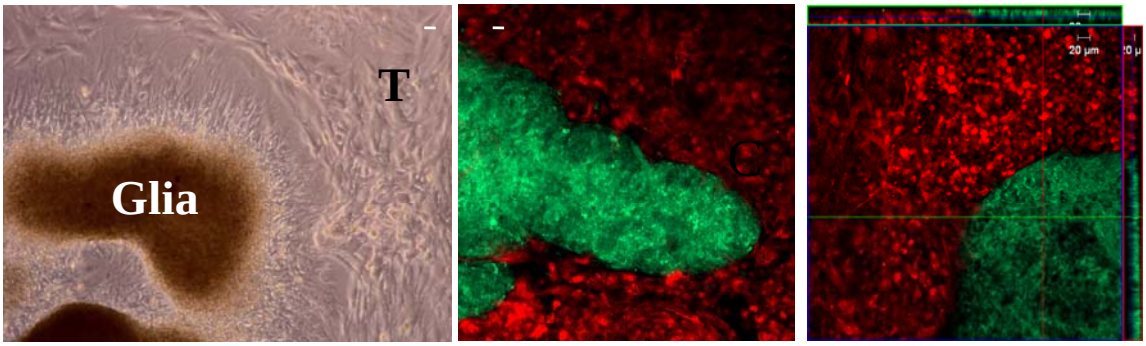

I= 1.8 I= 2.1

C

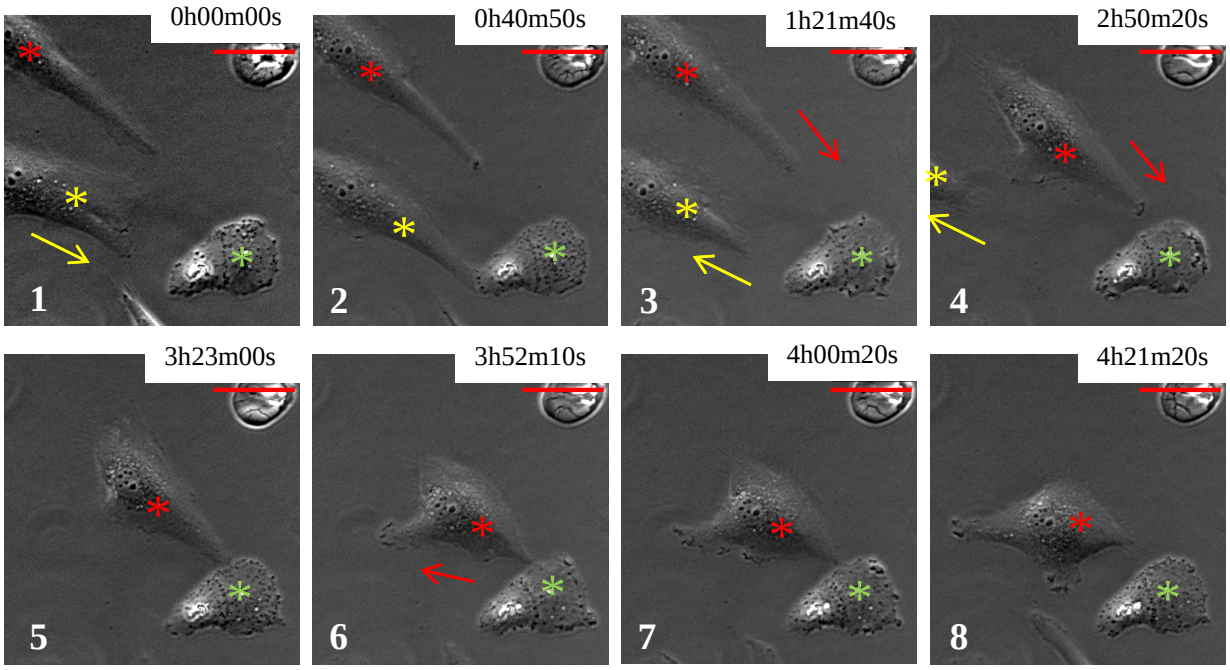

D

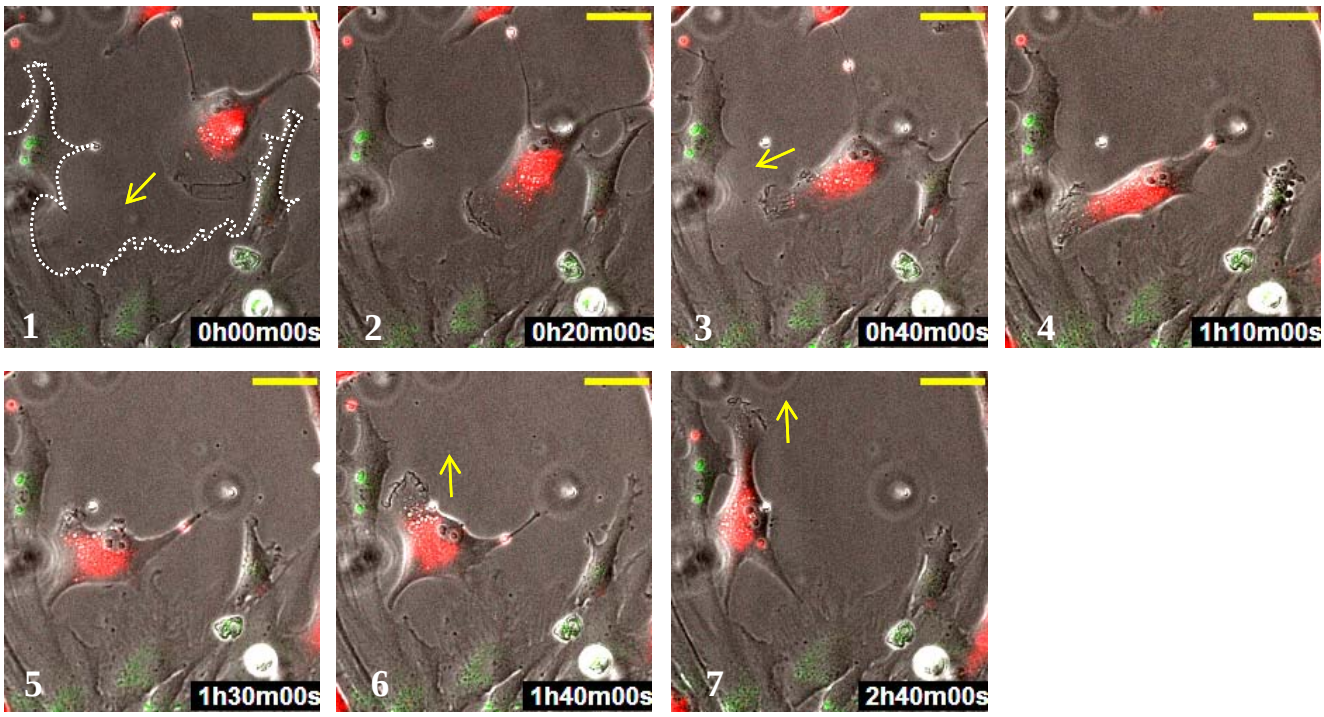

Fig 2

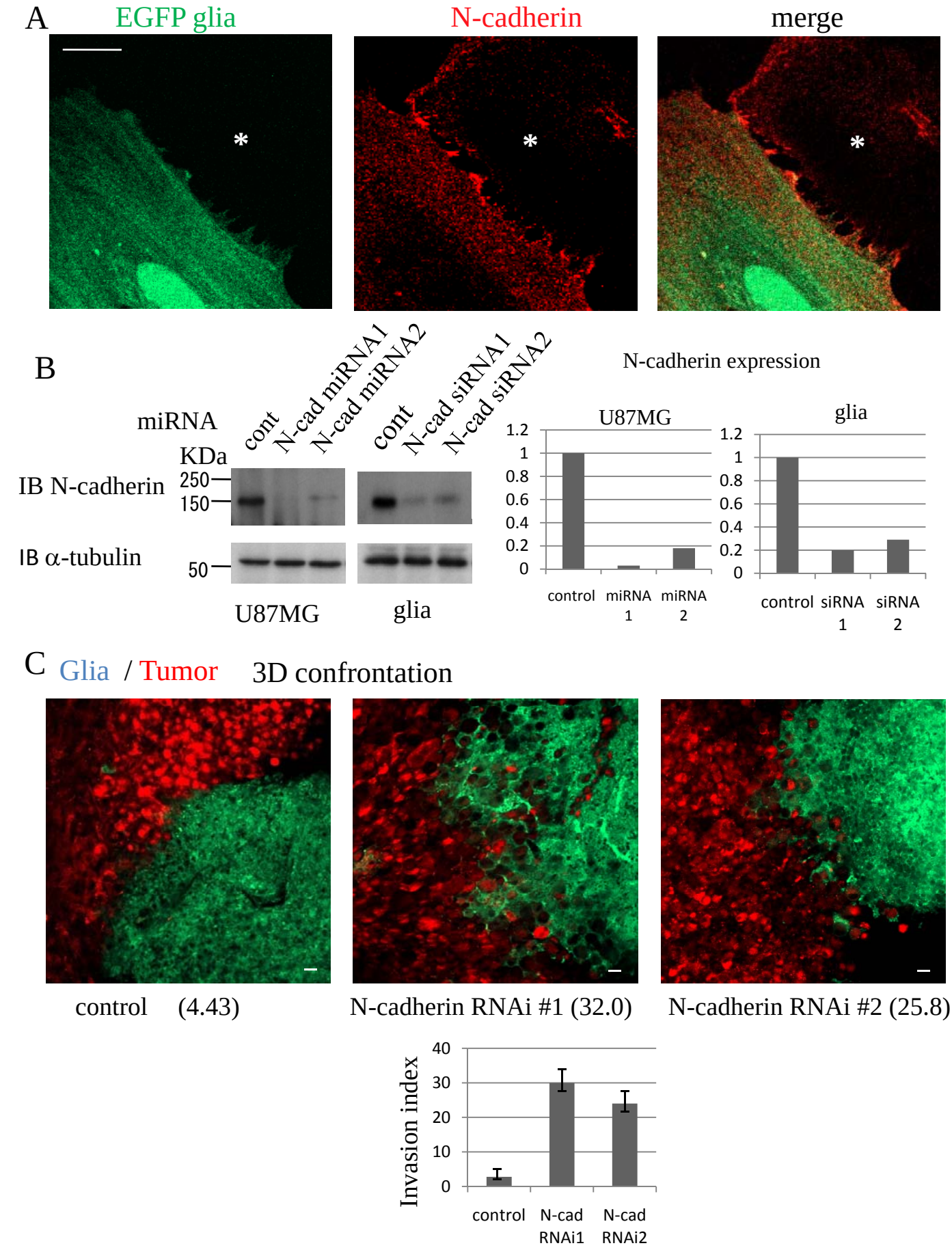

Fig 3

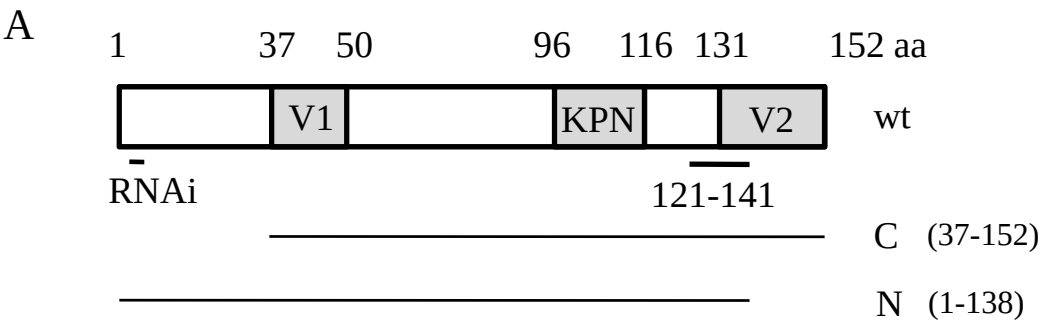

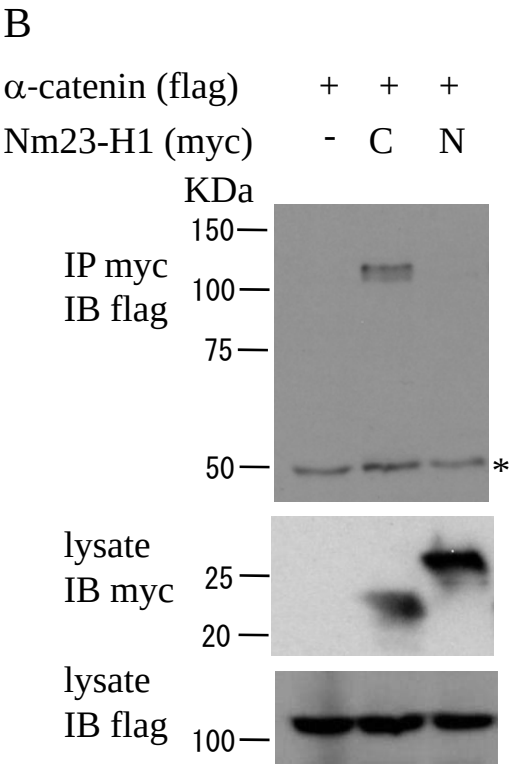

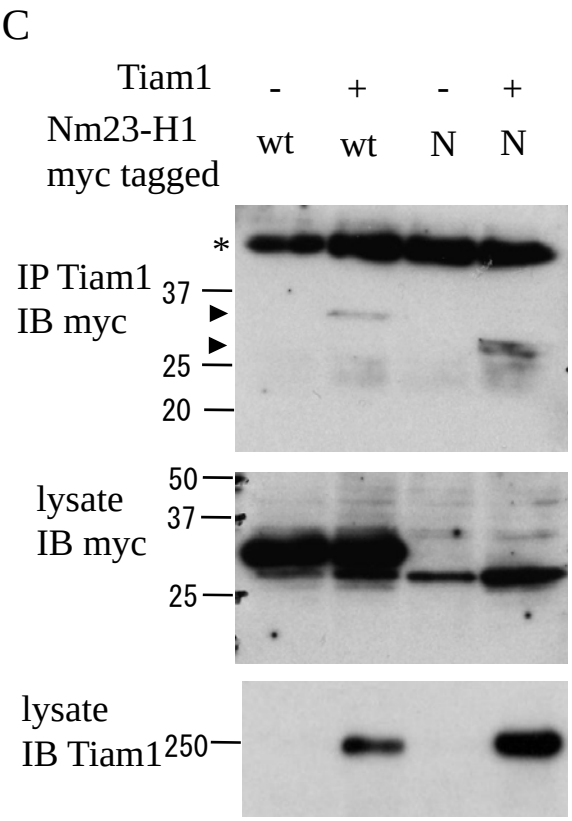

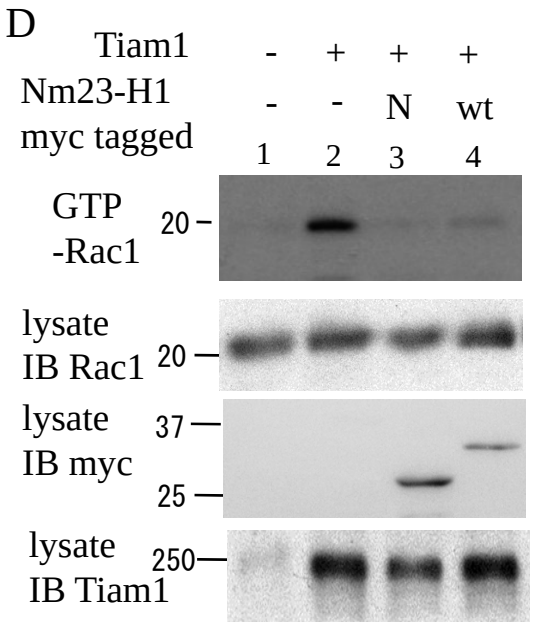

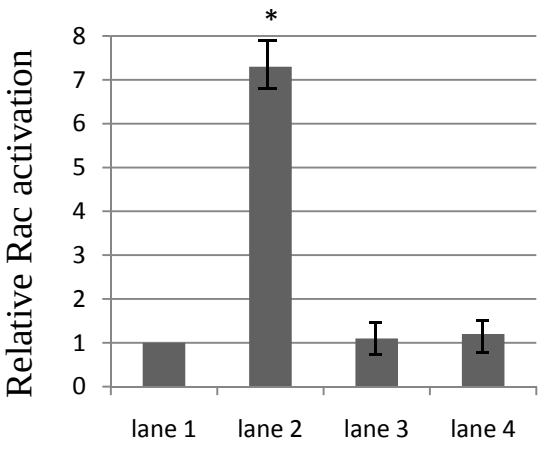

Fig 4

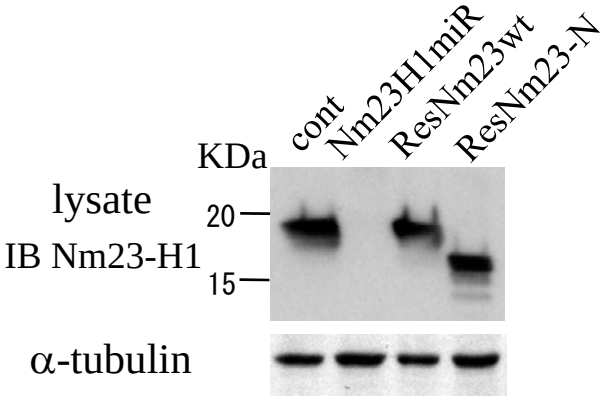

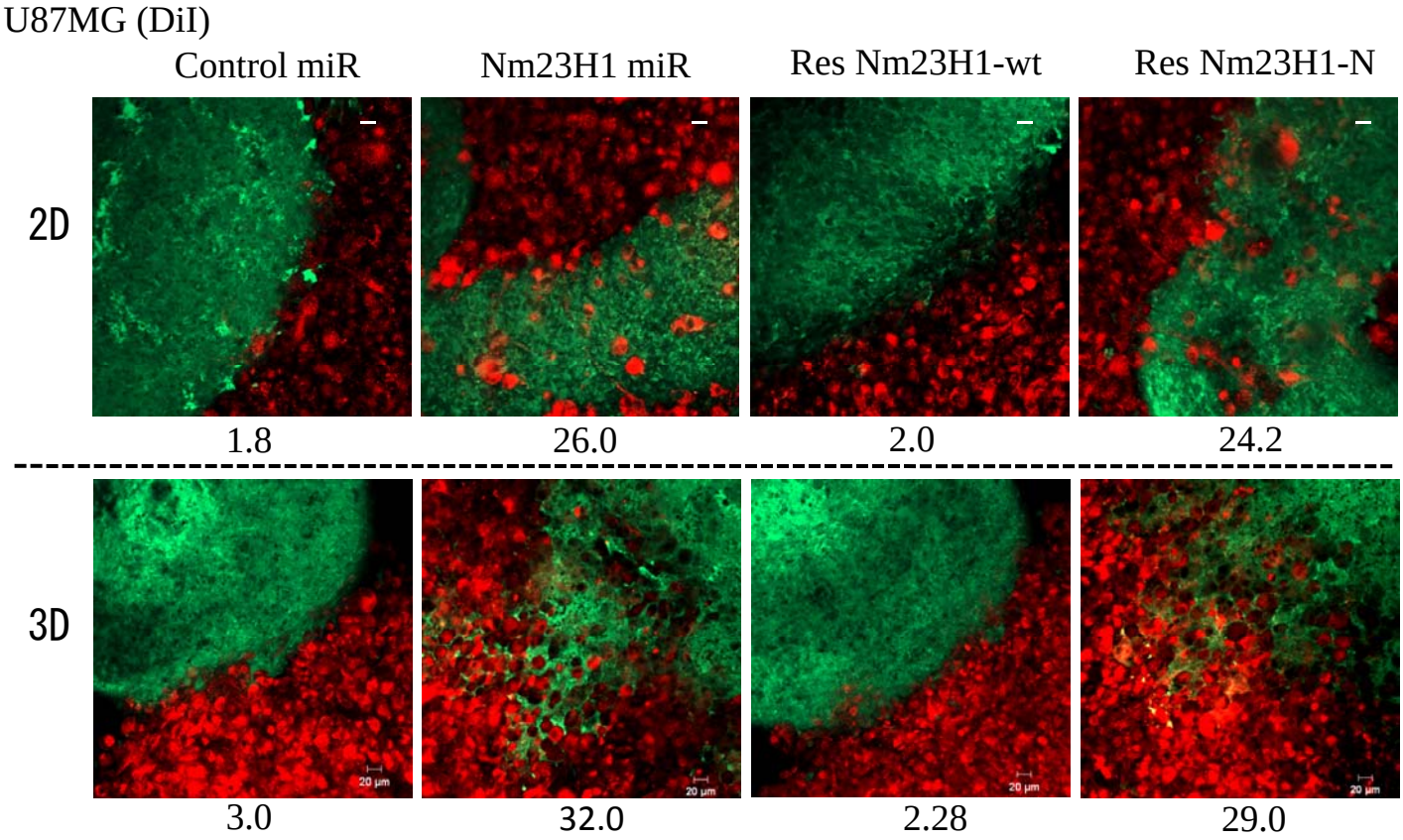

Fig 5

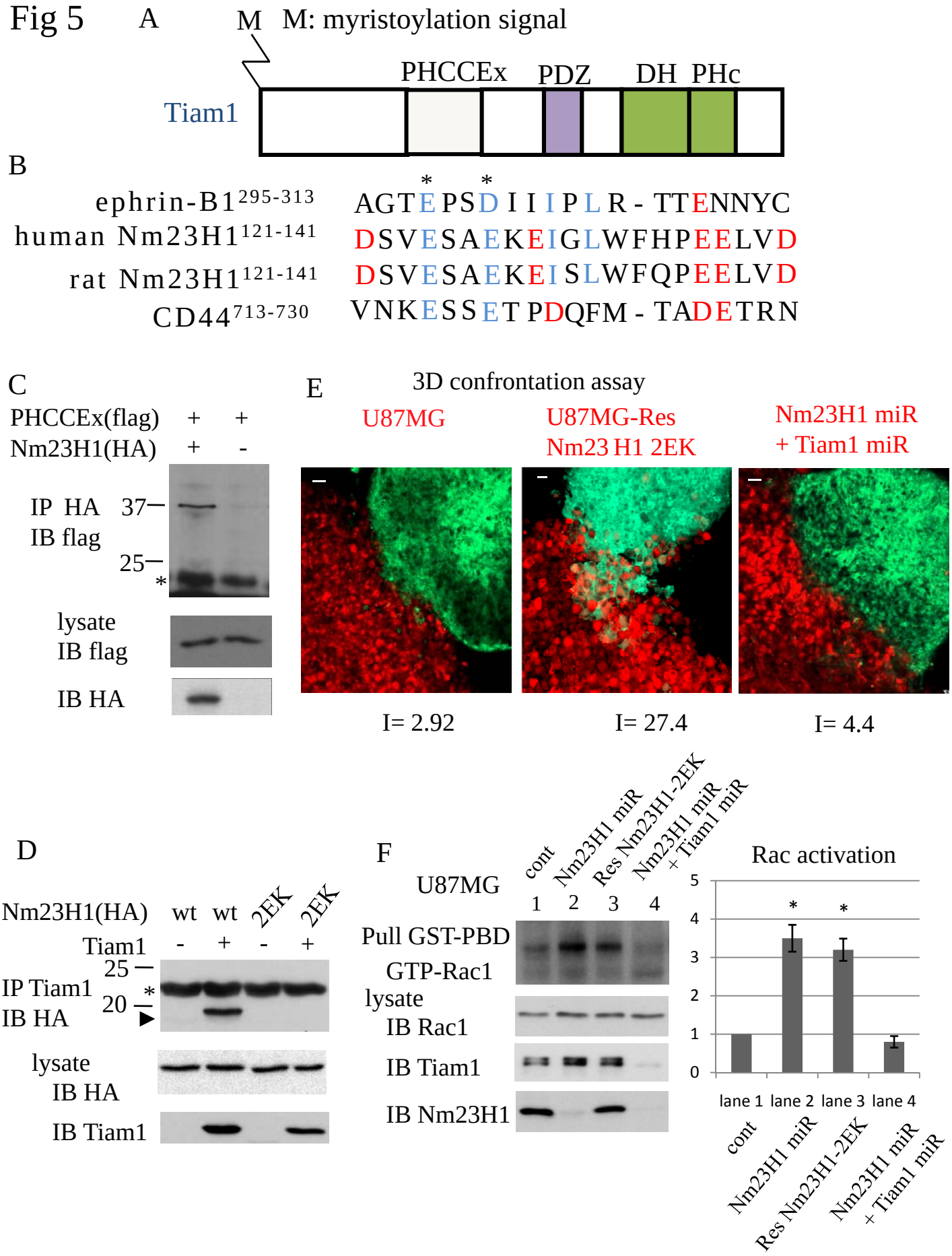

Fig 6

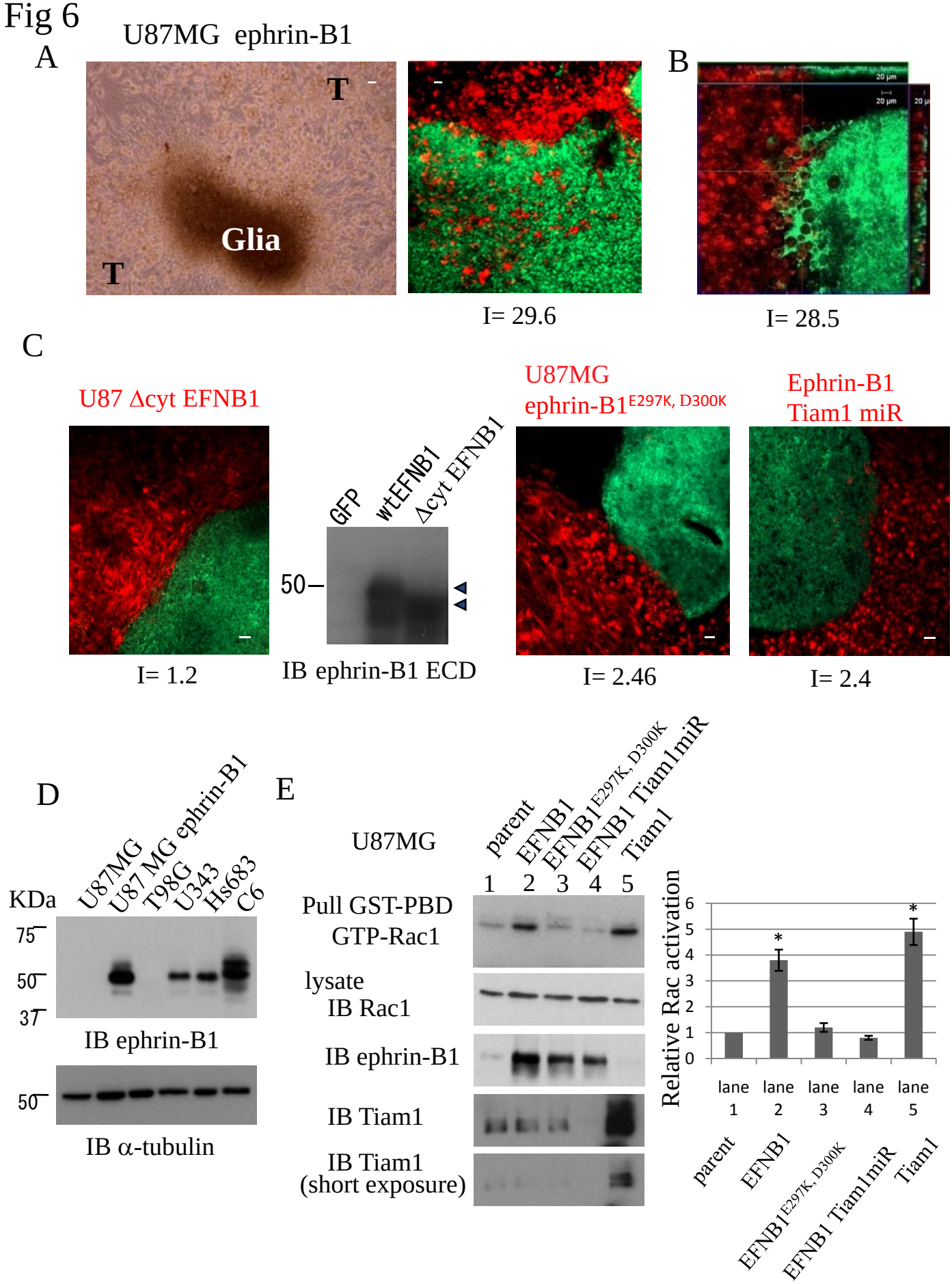

Fig 7

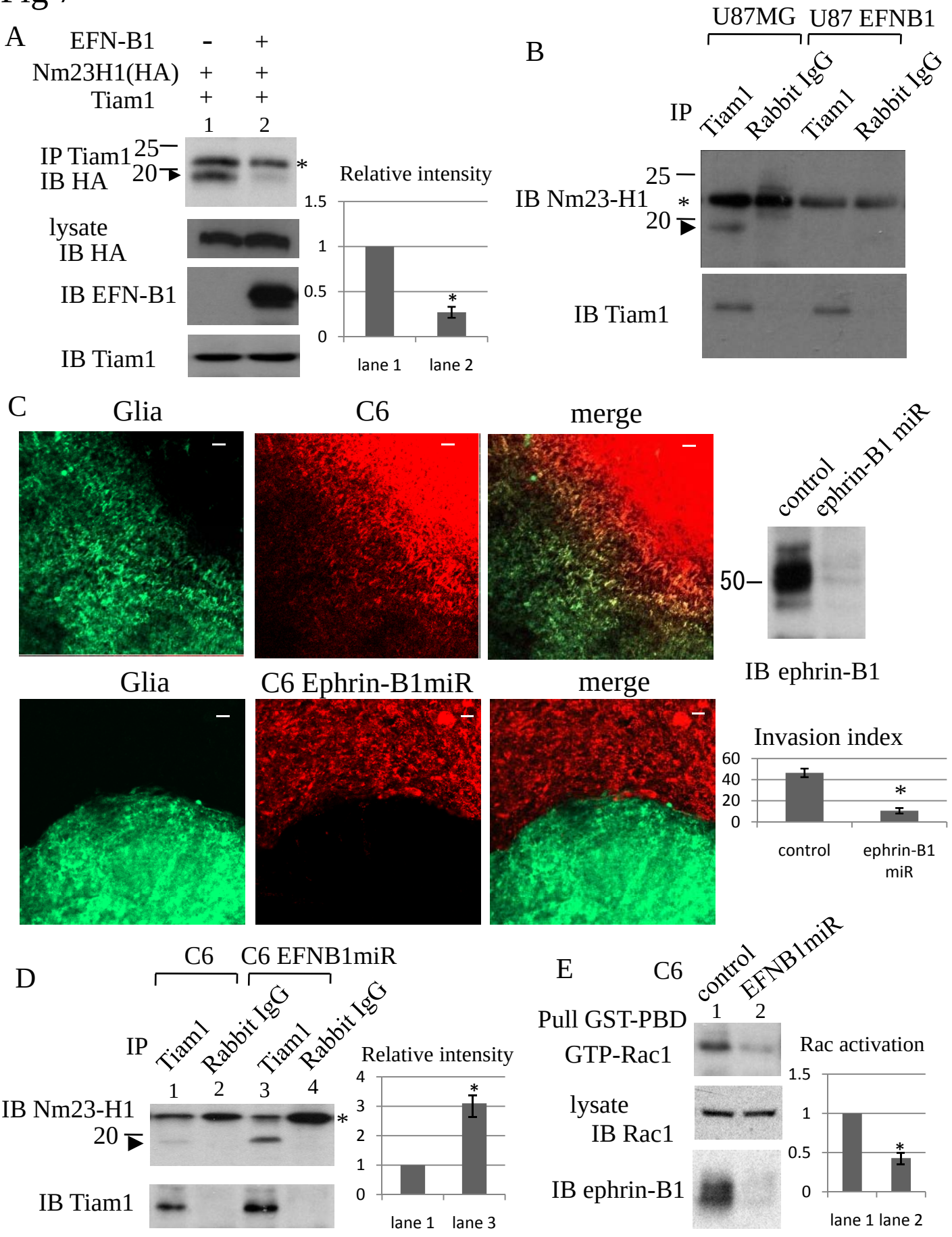

Fig 8

A

U87MG control

U87MG
ephrin-B1 overexpression

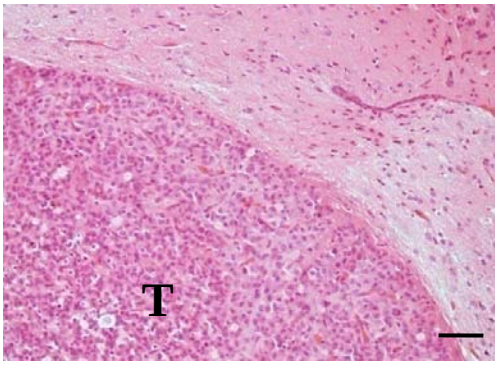

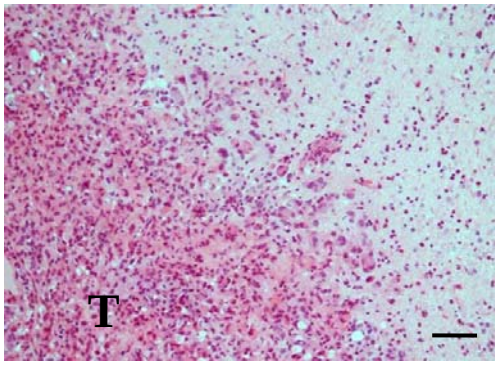

Ir = 1.05

Ir = 4.0

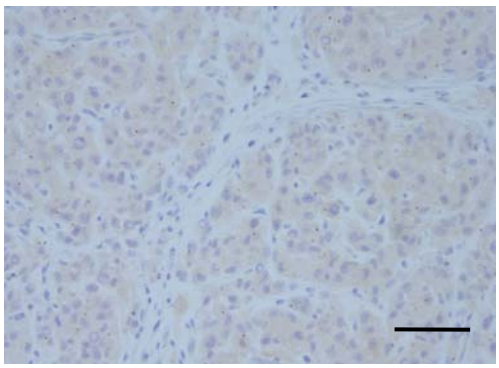

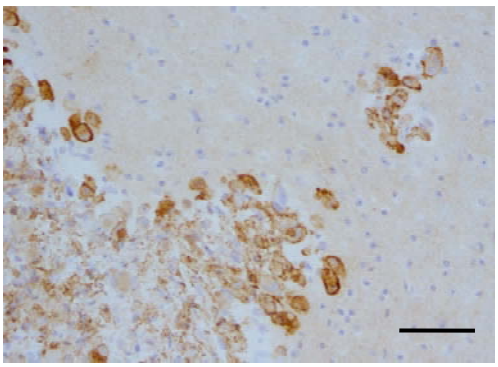

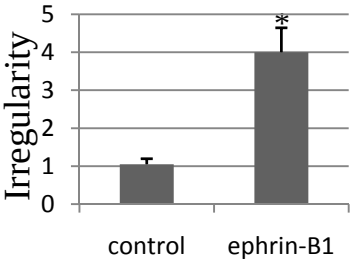

B

C6 control

C6 ephrin-B1miR

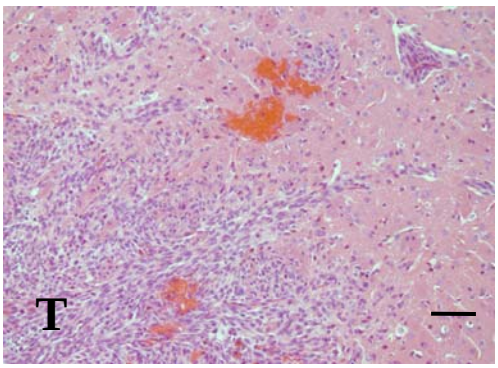

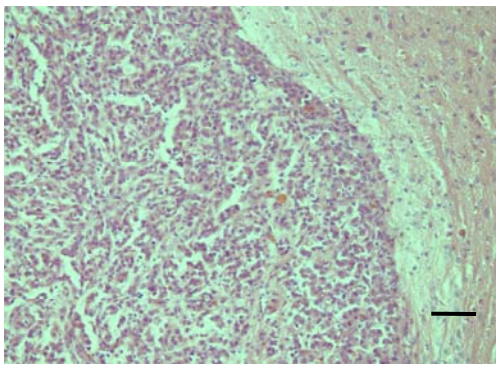

Ir = 3.49

Ir = 1.3